



Bioinspired silk fibroin materials: From silk building blocks extraction and reconstruction to advanced biomedical applications



Xiang Yao, Shengzhi Zou, Suna Fan, Qianqian Niu, Yaopeng Zhang *

State Key Laboratory for Modification of Chemical Fibers and Polymer Materials, Shanghai Engineering Research Center of Nano-Biomaterials and Regenerative Medicine, College of Materials Science and Engineering, Donghua University, Shanghai, 201620, People's Republic of China

ARTICLE INFO

Keywords:

Building blocks extraction
Regenerated silk fibroin material
Cell-material interaction
Soft tissue engineering
Flexible bioelectronic device

ABSTRACT

Silk fibroin has become a promising biomaterial owing to its remarkable mechanical property, biocompatibility, biodegradability, and sufficient supply. However, it is difficult to directly construct materials with other formats except for yarn, fabric and nonwoven based on natural silk. A promising bioinspired strategy is firstly extracting desired building blocks of silk, then reconstructing them into functional regenerated silk fibroin (RSF) materials with controllable formats and structures. This strategy could give it excellent processability and modifiability, thus well meet the diversified needs in biomedical applications. Recently, to engineer RSF materials with properties similar to or beyond the hierarchical structured natural silk, novel extraction and reconstruction strategies have been developed. In this review, we seek to describe varied building blocks of silk at different levels used in biomedical field and their effective extraction and reconstruction strategies. This review also present recent discoveries and research progresses on how these functional RSF biomaterials used in advanced biomedical applications, especially in the fields of cell-material interactions, soft tissue regeneration, and flexible bioelectronic devices. Finally, potential study and application for future opportunities, and current challenges for these bioinspired strategies and corresponding usage were also comprehensively discussed. In this way, it aims to provide valuable references for the design and modification of novel silk biomaterials, and further promote the high-quality-utilization of silk or other biopolymers.

1. Introduction

As a natural fiber material, silkworm silk, usually from *Bombyx mori* (*B. mori*) silkworm, has been used in home textile, clothing and even decoration industries for thousands of years because of its lightweight, high mechanical strength, good flexibility and luster. In addition, the *B. mori* silkworm is convenient for large-scale breeding and hence makes the silkworm silk could be easily obtained, which presents obvious advantages compared with other kinds of natural and industrialized synthetic biomaterials. Along with its good biocompatibility and biodegradability, silkworm silk has also been used clinically as biomedical suture material, as well as traditional cosmetics and healthcare products for a few hundred years [1,2]. Based on the effective clinical performance, the FDA (US Food and Drug Administration) has already approved the degummed natural silk as a biomaterial in 1993, especially for sutures and as a support structure during reconstructive surgery [3,4].

On the microscopic level, the morphological features of *B. mori* silk fiber presents an obvious core-shell structure, with an inner core of silk

fibroin (SF) and an outer shell of silk sericin (SS, a kind of glue-like protein). As for the biomedical application of silkworm silk, some immune rejection responses have been reported. Following studies have revealed that the contamination from residual sericin was the possible reason [2,5]. Therefore, thoroughly removal of sericin from silkworm silk is necessary to obtain non-immunogenicity SF biomaterials. Many recent researches on non-sericin contained silk materials, also denoted as degummed natural silk and regenerated silk fibroin materials, have illustrated that the independent SF exhibit comparable cytocompatibility *in vitro* and biocompatibility *in vivo* with other commonly used biomaterials such as collagen and polylactic acid [6,7].

As a protein fiber with hierarchical structure and fixed diameter, it is difficult to directly prepare materials with other formats except for yarn, fabric and nonwoven based on the degummed natural silk, which obviously limited its application scenarios and fields. In order to solve this issue, a promising bioinspired strategy is first extracting the desired building blocks of degummed natural silk, then reconstructed them into functional regenerated silk fibroin (RSF) materials with varied formats

* Corresponding author.

E-mail address: zyp@dhu.edu.cn (Y. Zhang).

including microspheres, fibers, films, electrospun mats, hydrogels, and 3D porous scaffolds etc. [2,8,9]. This bioinspired indirect approach could give RSF material excellent processability and easy to be combined synergistically with other biomaterials to form biopolymer composites, which could well meet the diversified needs and hence has been intensively investigated for usage in different biomedical applications.

It is well known that the function and property of material are much dependent on its structures [10–12]. As for the SF, it presents a natural hierarchical structure formed by bundles of silk microfibril. Our previous report has revealed that the microfibril is further formed by spontaneous nanofibers, which are composed of silk nanoribbon (SNR). And corresponding SNR is constituted by interval distributed random coil and β -sheet structures of the SF molecule [13], as schematically shown in Fig. 1A. The folding conformation specifies the excellent inherent

properties of silk fibers. Further structural analysis illustrated that the formation of different secondary structures is closely related to the primary sequence of amino acid in the SF molecule. The long-concatenated hydrophobic domains in *B. mori* SF are mainly composed of the repetitive blocks of $(GA)_nGX$ motifs, which induce the ordered structures and generate crystalline or semi-crystalline regions [7,14]. For example, the highly repetitive GAGAGS hexapeptide sequences generate the anti-parallel β -sheets and form crystalline domains [15]. The less repetitive GAGAGY blocks constitute the type II β -turns and form the semi-crystalline regions. The GAAS and GAGS sequences generally form β -turn structures. The non-repetitive hydrophilic motifs will constitute less ordered structures to form amorphous domains [15]. In the influence on mechanical properties, various reports have revealed that the anti-parallel β -sheet domains play an important role in determine the

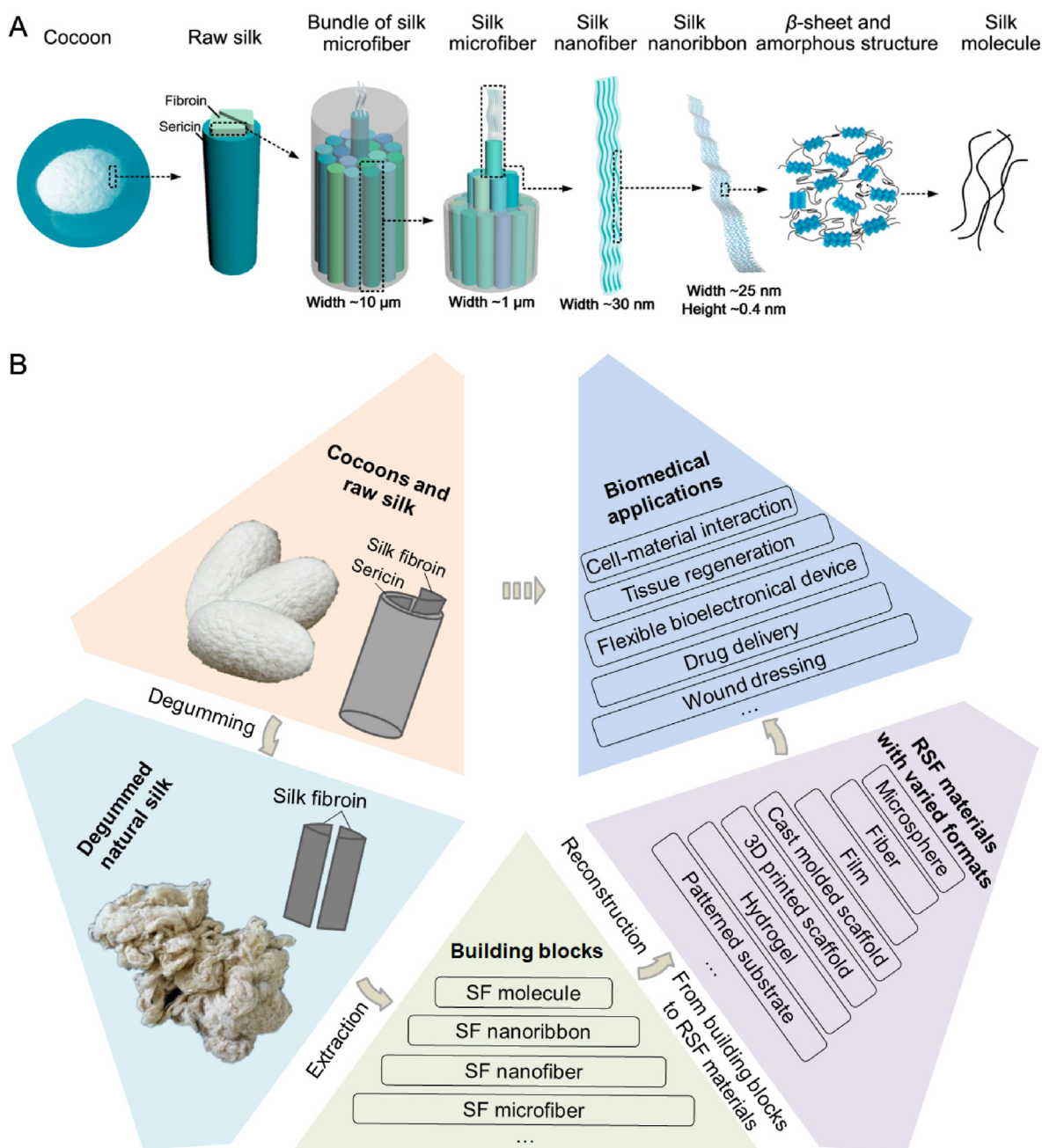


Fig. 1. Schematic presentation of the hierarchical structure and bioinspired usage strategies of natural silk. (A) Hierarchical structures of the natural silk. (B) Silk fibroin usage through the bioinspired indirect strategies: from silk building blocks extraction and reconstruction to biomedical applications. SF: silk fibroin, RSF material: regenerated silk fibroin material. Image (A) was modified with permission [13]. Copyright 2018, American Chemical Society.

excellent mechanical strength of silks by providing stiff ordered blocks, while the semi-amorphous structures which contains β -turn, helix, and random coil structures between crystalline domains provide remarkable elasticity of silk [7,16].

To engineer RSF biomaterials with desired function and raw silk-mimic or beyond mechanical properties, building blocks extraction process that could retain the original micro or nano structures, including the typical secondary structures of the natural silk have been desired. The reconstruction process is another important factor to determine the structure of corresponding RSF biomaterials and hence also profoundly influence their functions and properties. So, both the strategies of building blocks extraction and corresponding building blocks reconstruction are crucial processes to determine the comprehensive properties of functional RSF materials, such as the mechanical strength, flexibility, biodegradability, and even cytocompatibility.

In this promising bioinspired field, recently developed strategies have led to the transformation of extracted building blocks into a variety of novel biomaterials. The easily accessible of silkworm silk, clinical success of degummed natural silk sutures, and excellent processability of the RSF materials have also encouraged a recent expansion of biomedical application researches focus on RSF biomaterials. Majority of the RSF materials could be used for the basic study of cell-material interactions because of the good cytocompatibility and its convenient for various physical and chemical modifications [17,18]. Such as revealing the effects of macro or nano topological features [19], fiber arrangements [20], pore sizes [21], mechanical properties [22], and even material degradation process [23,24] on cell behaviors. Among these functional reconstructed biomaterials, RSF films are of particular interest for bio-electronic devices because of the transparency (over 90% transmission across the visible range) and flexibility [25–27]. RSF hydrogel, fiber mat, sponge and scaffold are of particular interest for both tissue engineering and wound dressing because of their tunable mechanical properties and biodegradability [28–30], and for drug release own to the available aqueous processing for silk building blocks [31]. As far as we known, besides silk surgical sutures, a few kinds of SF based biomaterials have also been successfully commercialized and applied in clinical treatment based on these basic researches. Such as the commercial products of SERI surgical stents (Serica Technologies Inc.), Silk Voice® injections (Sofregen Inc.), and special silk clothing for the treatment of skin diseases. It's believed that more and more SF based commercial products, such as wound dressing materials, surgical stents and porous tissue engineering scaffolds will be available in the near future.

Based on the commonality of these bioinspired fabrication and usage strategies of natural silk. This review provides an overview of controllable extraction of silk building blocks at desired levels (top-down), related powerful reconstruction strategies (bottom-up) and effective biomedical applications of the RSF biomaterials, as schematically illustrated in Fig. 1B. In the first part of the review, the developed fabrication technologies of desired silk building blocks at varied levels and related oxidation methods are highlighted. Following this section, recent advances in the controllable construction of functional RSF materials from silk building blocks are described. After that, advanced biomedical applications of the related RSF materials are also discussed, with a specific focus on the fields of cell-material interactions, soft tissue engineering, and flexible bioelectronic devices. Finally, potential study and application for current challenges and future opportunities for this bioinspired fabrication and application route are also comprehensively discussed. These relevant knowledges could provide valuable references for the design and modification of novel biomaterials, and further promote the high-quality-utilization of silk or other biopolymers.

2. Desired building blocks extraction

Until now, besides the traditional extraction of SF at molecule level, some novel extraction processes which retain partial of the original hierarchical structures of natural silk have also been developed in order to

maintain the excellent inherent properties of natural silk. As mentioned before, completely removal of sericin from silkworm silk is necessary to obtain non-immunogenicity SF biomaterials [2,5]. Thus, removing of the sericin has become the beginning process of the extraction for silk building blocks, which is also called degumming. During the degumming process, it is commonly used boiling Na_2CO_3 aqueous solution, NaHCO_3 aqueous solution, or urea solution to dissolve and remove the glue like sericin protein [2,32]. After that, the degummed natural silk was obtained for later building blocks extraction.

2.1. SF molecule

Due to the natural hierarchical structure, the obtained degummed natural silk couldn't be directly dissolved or separated in water for SF molecule or silk fragment extraction. Until now, the most popular way for SF molecule extraction is using proper chemical reagents to break the intermolecular hydrogen bonds between them. After dialysis for purification, the SF molecular solution could be obtained and feasibly for further reconstruction strategies, such as spinning, cross-linking, casting molding, 3D printing *etc.* Herein, the obtaining of high concentration of SF solution without insoluble aggregates is also quite important, as it determined the available reconstruction methods. For example, the 3D printing and biomimetic dry spinning both need SF solution with a high concentration.

The commonly used dissolution strategies to obtain SF solution are lithium bromide dissolution, calcium chloride-organic acid dissolution, and ionic liquid dissolution. The lithium bromide dissolving system is relatively slow, while the aqueous solution system in this method is environmentally friendly and non-toxic to biological system, thus quite suitable for biomedical applications [33,34]. The dissolving speed of calcium chloride-organic acid system is fast, but the usage of organic acid release pungent odor and need a relative long time to remove relevant organic acid through volatilization [35,36]. As for the ionic liquid, the inevitable residual of solvents is probably toxic to the cell and biological system [37,38] due to the non-volatility of ionic liquid.

In the field of SF molecule extraction for biomedical applications, the most valuable extraction methods are lithium bromide dissolution and calcium chloride-organic acid dissolution. For SF molecule extraction by lithium bromide [34,39], the degummed natural silk was usually dissolved in lithium bromide aqueous solution. After dissolving, insoluble components in the solution were removed by centrifugation and filtration. Then, the obtained solution was dialyzed against deionized water to remove salt and get a pure SF aqueous solution with relative lower concentration, as schematically illustrated in Fig. 2A, and then further slowly concentrated to the desired manufacture concentration at suitable conditions. For SF molecule extraction by calcium chloride-organic acid system [36,40], the degummed natural silk was usually dissolved in calcium chloride-formic acid mixed solution at room temperature. Then the solution was filtered to remove the impurities. Because the solvents used in this strategy are toxic for cells, it need to be vacuum dried at least 2 days to fully remove the solvents from the intermediate products or final constructed RSF materials. An ideal extraction method of SF molecule should effectively break the connections between molecules while not destroy the structure of polypeptide chain. Different extraction conditions could change the yield and molecular weight of SF molecule, and further affect the physicochemical property and biological activity of the obtained RSF material to some extent. Therefore, it is an important development direction to find a nontoxic, mild, and controllable extraction strategy in this field.

2.2. SF nanofiber or microfiber

SF protein in silkworm silk is a natural hierarchical structure formed by spontaneous nanofibers, which is mainly constituted by interval distributed random coil and β -sheet structures. The folding conformation specifies the excellent inherent properties of silk fibers. Obviously, for the

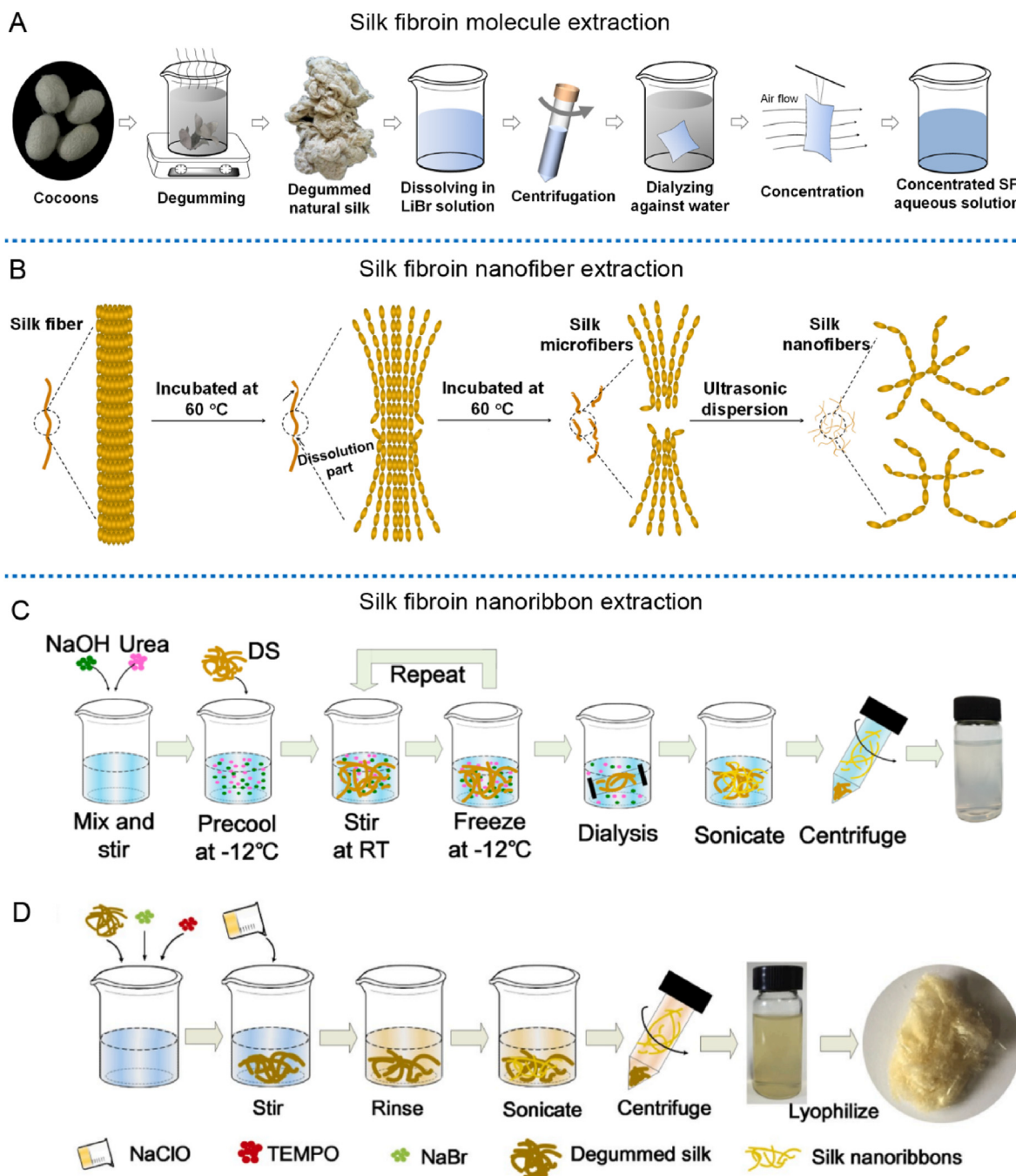


Fig. 2. Schematical illustration of the extraction procedures of the building blocks of silk at different levels. (A) SF molecule extraction using lithium bromide dissolution. (B) Solvent and ultrasound assisted extraction of SF nanofibers. (C) SF nanoribbons (SNR) extraction process using NaOH/urea solvent system. (D) SNR extraction process using TEMPO/NaBr/NaClO solvent system. Image (C) was reproduced with permission [13]. Copyright 2018, American Chemical Society. Image (D) was reproduced with permission [41]. Copyright 2020, Elsevier Ltd.

researchers concerned, the acquisition of silk nanofibers partially containing the functional structure elements is very attractive.

In this research field, Zhao et al. [42] have attempted to peel nanofibers from natural silk by high intensity ultrasound treatment. Although the nanofiber can be stripped from the hierarchical structure of polysaccharides such as cellulose and chitin, it is very difficult to extract expectant SF nanofibers because of the complex and dense structure of natural silk. Besides, the nanofibers prepared by this mechanical extraction method cannot be stably dispersed in the solvent system.

As mentioned in section 2.1, it is known that proper solvent can effectively break the interconnections between SF molecules. In recent

years, by integration of the partial dissolution and mild ultrasonic dispersion methods, the SF nanofibers have been successfully extracted. For example, during the hexafluoroisopropanol (HFIP) incubation, the HFIP gradually permeated into the degummed natural silk and partially dissolved the silk from defects and ends, inducing SF microfibril or dispersed nanofibril with the combination of mild ultrasonic dispersion [43,44], as schematically illustrated in Fig. 2B. In addition, other oxidation methods based on this basic strategy have also been developed to make the nanofibers extraction more feasibly. For instance, the nanofibers prepared by TEMPO (2,2,6,6-tetramethyl-piperidine-1-oxyl radical) catalytic oxidation method retained the crystal structure of the

natural silk and presented higher aspect ratio. Moreover, the carboxyl group on the surface of the prepared nanofibers is formed by the oxidation of hydroxymethyl, and the negatively charged single nanofibers can be more stably dispersed in the solvent system [45]. In addition, some other strategies have also been developed to extract SF nanofibers, such as the combination of milling and homogenization approach, and the green deep eutectic solvent (DES) treatment assisted by mild mechanical disintegration [46,47].

Except for nanofibers, the controllable and repeatable extraction of microfibrils that retain partial of the inherent structures of the natural silk have also been desired and developed, which is usually based on chemical stripping, such as hydrolysis of degummed natural silk into microfibrils [32,48]. For hydrolysis of degummed natural silk, sodium hydroxide solution was generally used. After that, excessive distilled water was used to stop the hydrolysis and then centrifuged. The obtained microfibrils were then resuspended and centrifuged to remove excess remaining alkali. To obtain longish (400–500 μm long) and medium (150–200 μm long) microfibrils, the hydrolysis reaction could be carried at room temperature for about 30 s and 180 s, respectively. To obtain shorter (10–20 μm long) microfibrils, the reaction mixture could be placed in a boiling water bath for about 60 s to induce intense hydrolysis [32].

2.3. SF nanoribbon

Another silk building block between the scale of SF molecule and SF nanofiber is SNR, as schematically shown in Fig. 1A. Recently, by using appropriate solution and processing, Niu et al. have firstly extracted this unique SNR with retained inherent silk features [13]. Briefly, a mixed solution of NaOH and urea in deionized water was prepared and then precooled. The degummed natural silk was then immersed into the mixed solution. Related suspension was stirred at room temperature. Next, the suspension was dialyzed [13], then sonicated in ice-water. The SF nanoribbons dispersion could be obtained by centrifugation after corresponding sonication, as schematically shown in Fig. 2C. The width and thickness of the SNR were about 21.8 nm and 0.44 nm, respectively. Moreover, the thermostability curve, types and mass ratio of amino acids for the extracted SNR are quite similar to those of degummed natural silk, which hinted that this kind of SNR probably retained the basic features of natural silk.

Alternatively, another method for SNR extraction have also been developed by changing corresponding oxidizing solvent system [41]. In brief, appropriate mass ratio of degummed natural silk, NaBr and TEMPO were suspended in deionized water, then added proper amount of NaClO to initiate the oxidation. The oxidation reaction was stopped when the pH remained constant. After that, the salts and dissolved SF molecule were removed by rinsing the mixture with deionized water. The final mixture was sonicated in ice water and centrifuged. Finally, SNR could be harvested from the supernatant of the centrifuged samples [41], as illustrated in Fig. 2D. Characterizing of the SNR illustrated that the width and thickness are about 20.2 nm and 0.4 nm, respectively. Compared with NaOH/urea solvent system, TEMPO/NaBr/NaClO solvent system presents more advantages, such as energy saving, simpler experiment operation, more stable suspension, and higher yield of SNR.

In the field of nanofiber or nanoribbon fabrication, in order to enhance the stability of the building blocks suspension, a promising method is to oxidize corresponding products. The oxidation could effectively change hydroxymethyl group into carboxyl group, thus introducing negatively charges on the silk building blocks of silk fibroin nanoribbons and nanofibers. Thus, the resultant electrostatic repulsions between silk building blocks facilitates the dispersion and offers higher stability of silk fibroin nanoribbons and nanofibers. This kind of modification offered much benefits for the storage, transportation, and engineering applications of these products. Specifically, it could firstly oxidize the degummed natural silk and then extract corresponding

building blocks of the modified silk fiber, or firstly extract the building blocks from degummed natural silk and then directly oxidize the obtained building blocks. As for the oxidization agent, except for NaClO system, another commonly strategy is TEMPO-mediated oxidation. For more detail information about these oxidation strategies, some pertinent literature [45,49,50] are recommended. Based on this guidance, a few strategies about directly oxidize the building blocks such as SF molecule have also been attempted [45].

3. From building blocks to RSF materials with controllable formats and structures

After obtain the basic structure elements of degummed natural silk, the reconstruction strategy of corresponding building blocks is another important process to regulate the formats, structures, and functions of RSF materials, which will be detailly described in this section. Once the obtained building blocks are processed into RSF materials, the final stage is often to induce crystal structures in RSF materials for water insolubility. The crystal structure was commonly induced *via* two methods, either by immersion in an alcohol or by water vapor annealing [51,52]. Among them, alcohol such as methanol or ethanol solution treatment is simple and fast. While if some sensitive chemicals (such as growth factors) need to be loaded, the mild water vapor annealing should be considered. Water vapor annealing is the process in which the RSF materials are incubated in a humid environment with a relative humidity higher than 95%.

3.1. RSF microsphere

In general, the constructed RSF microspheres could be used to encapsulate and release growth factors or therapeutic compounds in the biomedical applications. A popular fabrication procedure is using phase separation between SF and another appropriate polymer, such as polyvinyl alcohol (PVA) [53]. Briefly, an appropriate concentration of SF aqueous solution needs to be firstly prepared. Then drop the solution into PVA solution, mix them gently and disperse thoroughly with a low-power ultrasound. During this process, the SF molecule in the mixed solution will undergo phase separation to form a microsphere structure spontaneously. Then pour the mixture onto a substrate to form a film and then dissolve the PVA component with deionized water. After centrifugation, RSF microsphere could be obtained [53]. Microspheres with a diameter of about 300 nm - 20 μm could be fabricated by this method [53]. On account of the avoidance of organic solvents, active growth factor or drugs could be encapsulated in these microspheres by adding them into the SF solution prior to mixing with the PVA.

To ensure the biocompatibility of the whole system, a useful polyethylene glycol (PEG)-assisted emulsification method has also been developed to fabricate RSF microsphere [54,55]. By mixing SF solution with PEG, SF molecules would be separated into different segments by the hydrophilic PEG molecules, which further induced water-insoluble RSF microsphere formation. As usual, the mixed solution was incubated overnight at room temperature, followed by centrifugation to remove the PEG and non-encapsulated growth factors or drugs. In this process, the microsphere size could be well controllable by PEG molecular weight as well as PEG and SF concentrations, and larger sized (> 20 μm) microspheres could be obtained when compare to the PVA-assisted strategy. Both PEG and SF have excellent biocompatibility, so, this kind of method will be useful in a variety of biomedical applications. Recently, some other kinds of strategies have also been attempted to prepare RSF microspheres, such as the high-gravity anti-solvent precipitation method [56] and emulsion cross-linking strategy [57]. These studies have afforded different kinds of functional RSF microspheres and provided promising opportunities for the loading and sustained releasing of bioactive factors.

3.2. RSF fiber

The biological spinning gland of silkworm presents precise structure and exquisite silk forming mechanism. By using this natural spinneret, silk fiber with excellent comprehensive performance can be obtained at normal temperature and pressure. Biomimetic spinning by microfluidic chip refers to this structure and environment might obtain fiber materials with high performance and has become an important research topic in the construction of RSF fiber [58–60]. In addition, some conventional wet spinning and dry spinning methods have also been attempted to fabricate RSF fibers [61,62]. In the processes of biomimetic spinning by microfluidic chip, both the physical and chemical environment cues could be feasibly adjusted, which is expected to realize the multifunctional biomimetic integration of biological spinner, as schematically summarized in Fig. 3A.

In the early stage, microfluidic chip was mainly used to study the aggregation and assembly process of SF, and the used SF was only about 2 wt% in concentration, which was far from 30 wt% of spinning stock solution in silkworm gland [64]. Until 2011, Kaplan et al. achieved the wet spinning of SF solution for the first time by using a microfluidic chip with a cross shaped channel [65]. The external channel of the microfluidic chip was filled with polyethylene oxide (PEO) aqueous solution to simulate the hydrodynamics in the silkworm gland. The internal channel was filled with SF aqueous solution, which directly entered methanol through the channel outlet for solidification and combined with stretching post-treatment. Using this technology, RSF fiber with a breaking strength of about 70 MPa was fabricated [65], which was still far lower than that of the degummed natural silk, while this strategy promoted the development of microfluidic biomimetic spinning of RSF fiber. Then, Luo et al. designed a dual channel integrated microfluidic chip [66], introduced SF aqueous solution and PEG solution in the upper and bottom channels respectively. These two channels were separated by a regenerated cellulose membrane and successfully concentrated the SF

aqueous solution from 12 wt% to 31 wt% by using the water absorption properties of PEG. So, the biomimetic simulation of natural protein concentration process was achieved [66]. The same group [67] further took the single-stage exponential function as the design model to fabricate a microchannel with unique biomimetic channel features. Related exponential function can well describe the shape features of natural animal gland, and hence better simulates corresponding shearing and stretching effect. Combined with dry spinning technology, this study highly imitates the spinning process of silkworm for the first time. The RSF fibers obtained after post-treatment presented higher β -sheet content and higher degree of orientation than the degummed natural silk. The breaking strength and elongation were up to 614 MPa and 27% respectively [67]. These studies further confirmed the effectiveness and universality of the biomimetic spinning platform based on microfluidic chip.

Based on the above research basis, Zhang's group have also systematically studied the influence of spinning environment on RSF fiber properties and extended it to the preparation of coaxial fibers and composite fibers with hierarchical structures. For example, by introducing TiO_2 in the spinning process, a simple and cheap strategy to greatly toughen RSF fiber was achieved [63]. The toughness of the RSF fiber (breaking energy $93.1 \pm 27.1 \text{ MJ m}^{-3}$) exceeded that of natural silk, which was probably because of the nanoconfined crystallite toughening effect in hybrid RSF- TiO_2 fiber, as schematically shown in Fig. 3B. The hybrid fiber showed more random coils, fewer β -sheets, smaller crystallites and lower crystallinity than the pure RSF fiber, thus enhanced its toughness [63]. A new possibility of controlled design for hierarchical protein based materials was proposed by this finding. In addition, by introducing cellulose nanofibers (CNF) into SF solution, RSF/CNF composite fibers with greatly improved crystallinity and mechanical properties have been prepared by taking advantages of the CNF orientation and its effective interaction with RSF molecules during the biomimetic microfluidic chip spinning [58,59], as illustrated in Fig. 3C. The breaking strength of the RSF/CNF fibers could increase to $486 \pm 106 \text{ MPa}$ [58].

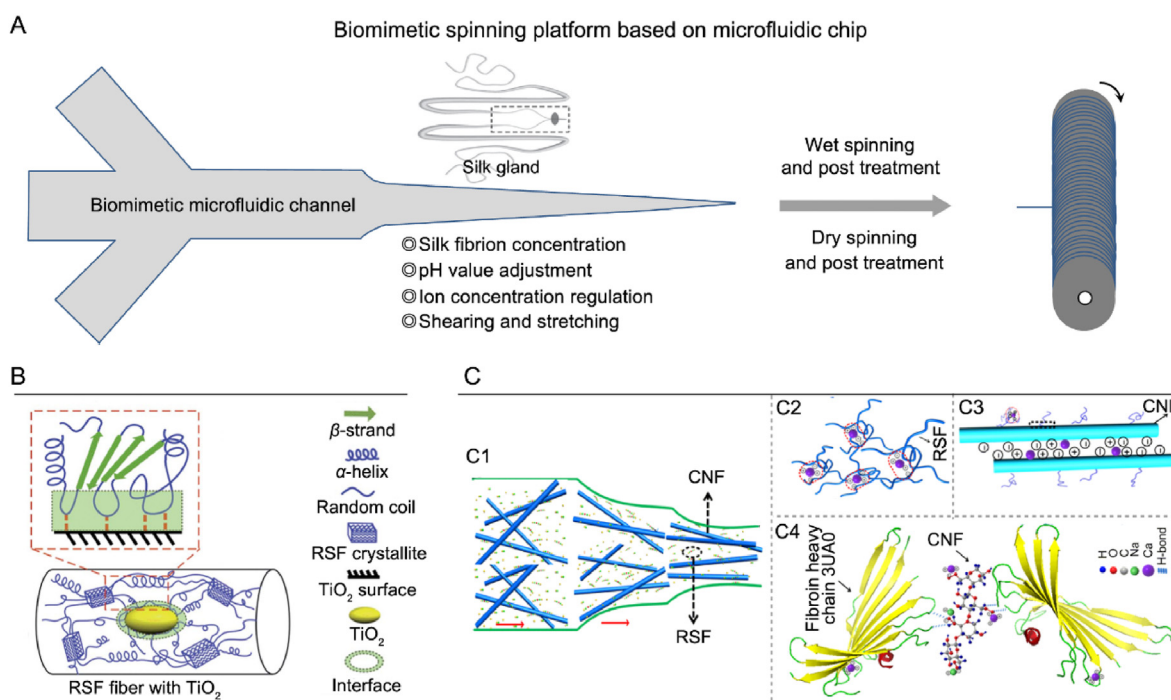


Fig. 3. Biomimetic spinning of SF by microfluidic chip to fabricate functional RSF fibers with hierarchical structures. (A) Design strategy and summarized properties of the microfluidic biomimetic spinning. (B) Mechanism model of the nanoconfined crystallite toughening effect in hybrid RSF- TiO_2 fiber. (C) Mechanism model of the nanofiber enhancing effect in hybrid RSF/CNF fiber. (c1) Hypothetical process of the orientation assembly of RSF/CNF through the microfluidic channel. (c2) Cross linking between SF molecular chains (dashed red circles). (c3) Interactions between SF molecular chain and the CNF with carboxyl groups (negative charge). (c4) Interfacial forces between the amino groups of SF molecule and carboxyl groups of CNF in the black square region in (c3). Image (B) was modified with permission [63]. Copyright 2014, The Royal Society of Chemistry. Image (C) was modified with permission [58]. Copyright 2019, American Chemical Society.

Interestingly, by wet spinning process using a biomimetic microfluidic chip which mimicking the shape of spider's major ampullate gland, a RSF/CNF hybrid fibers with high crystallinity, high mesophase content and small crystallite size was also fabricated recently by the same group [60]. Besides the high break strength (as high as 710 ± 33 MPa), this fiber also showed a low light loss of 1.0 dB/cm, which was much lower than that of degummed natural silk and most commercial biodegradable waveguides, and hence shown great application potential in the field of photodynamic therapy for deep tissue [60]. These useful biomimetic spinning strategies have afforded varied kinds of functional RSF fibers. Moreover, these studies and corresponding insights could also provide new strategies for the design and preparation of other high-performance man-made fibers with hierarchical structures.

3.3. RSF film

Conventional RSF film and electrospun RSF fiber mat could both be regarded as film material, which are mainly used as dressing, soft tissue repair, or flexible bioelectronic materials. In addition, this kind of material is also very powerful for revealing cell-material interactions with or without surface modification. Using the building blocks solution or dispersion, RSF film could be constructed by casting, vacuum filtration, and coating methods. RSF electrospun fiber mats could be feasible obtained by different electrospinning strategies.

The casting method for film fabrication is casting the SF based solution into the mold with relative flat bottom, then spread it evenly by gently shaking and tilting [2,68]. In order to maintain the fabricated film with uniform thickness, a level gauge was suggested to adjust the level of the mold. It's also important to fully expelling bubbles during the casting process. Another typical method is using vacuum filtration to prepare RSF film [41,43]. This strategy must need an appropriate filtration membrane such as polycarbonate membrane to interception the solutes with relative larger sizes, which is quite suitable for the raw material with suspension state. The casting and vacuum filtration methods have been widely used to prepare SF based films because of their simplicity. However, the films prepared by these methods are usually present relative larger thickness.

The coating method is just used for preparing RSF films with thinner thickness, which commonly contains spin coating and dip coating [69,70]. The spin coating is based on the principle of photoresist film formation in the photolithography technique. When dropping proper amount of SF-based solutions onto the substrate fixed on the spin coater, a uniform thin RSF film could be formed on the substrate under the rotating condition. The dip coating is immersing a suitable substrate into the SF based solutions, then pull it up at a certain speed. During this process, a thin RSF film could be formed on the substrate. The film thickness could reach about a few hundred nanometers using these kinds of coating strategies, while it needs SF based solutions with relatively higher viscosity for successful coating.

Compared with casting, vacuum filtration, and coating methods, the advantage of electrospinning is that it could fabricate films (fiber mats) with ECM-mimicking nanofiber structures, which were much suitable for inducing cell adhesion, proliferation, and function maintenance [71–73]. However, the electrospinning of RSF mats depends on toxic organic solvents for a long time, and also has the problems of poor spinnability and weak mechanical properties [74]. So, the using of nontoxic aqueous solution for electrospinning have been required and attempted [75,76], then gradually become a popular way for the preparation of biomedical RSF fiber mats, as schematically show in Fig. 4A. In order to resolve the common issue of the weak mechanical property of corresponding RSF fiber mats, Pan et al. used composite reinforcing phases for coaxial electrospinning [77], and also developed a method of combining ethanol post-treatment and mechanical stretching technologies to prepare RSF fiber mat, which could enhance its breaking strength as high as 8.6 MPa when compare to the 1.8 MPa of corresponding as-spun RSF fiber mat [78]. Because the ethanol post-treatment and mechanical stretching

could effectively improve the crystallinity and alignment of corresponding fibers. Recently, by choosing the regenerated *Antheraea pernyi* silk fibroin (RASf) with excellent inherent biocompatibility, Zou et al. firstly used conductive meshes as collectors to prepare electrospun RASf fiber mats from its aqueous solution [79], as schematically shown in Fig. 4B. Interestingly, compared to the traditional intact plate, a proper 7 mm gap sized mesh collector could not only significantly increase the pore size and porosity (see Fig. 4C–D), but also obviously enhance the elastic modulus and breaking strength (see Fig. 4E) of the fiber mats (RASf-7 mmG). Compared to the uniform random fiber distribution collected by traditional intact plate, the mesh collector could regulate the fiber configuration significantly. Specifically, the fibers in region II (near the non-cross-point zone of metal wires) arranged much densely and presented parallel orientation along with the underneath metal wires, while the fibers in region III (the gap zone of metal wires) arranged randomly and much sparsely (see Fig. 4B). So, the simultaneously enhanced porosity and mechanical properties were probably own to the comprehensive effects of the induced highly oriented arrangement of fibers in region II and the sparse arrangement of fibers in region III of the fiber mat (see Fig. 4B) [79].

In addition, the electrospinning technique could also be used to fabricate aligned RSF fiber mats by using round roller collector [31], as schematically shown in Fig. 4F. Moreover, combined with coaxial spinning technology, it could feasibly to alter the component of fiber shell and core parts or load different active factors, so as to fabricate fiber mats with controllable core-shell structures and achieve programmed release of different active factors [31]. The insight of these studies may also provide universal guidance for regulating the morphological features and mechanical properties of other electrospun fiber mats.

3.4. Cast molded RSF scaffold

3D scaffolds with porous structure are useful for the repair of specific tissue defect, especially for relative large-scale coloboma. At present, the commonly used construction methods for 3D RSF scaffold are cast molding and 3D printing technologies. Cast molding assisted with salt leaching or lyophilization method could be used to effectively fabricate 3D porous RSF scaffold. These two assisting approaches could also combined together to prepare scaffold with more hierarchical pore structures [80].

In the cast molding with salt leaching [81], it firstly needed to combine the active factor and enhancement component (if needed), salt like pore forming agent (such as NaCl) with proper concentration of SF aqueous solution and mixed them homogeneously. Then pour the mixture into a 3D mold. After solvent volatilization and post treatment by alcohol solvent or high humidity environment, put the shape fixed material into the deionized water for salt leaching. Since the salt like pore forming agent will be easily dissolved into the deionized water, porous structures could be formed after salt leaching.

In the cast molding assisted with lyophilization [82,83], it needed to combine the active factor or enhancement component (if needed) with SF aqueous solution. Then pour the mixture into a 3D mold. After shape fixing, freeze the material at low temperature. As the ice crystal (act as porogen role) formed during the low temperature treatment in the material bulk will be sublimated in the freeze-drying stage, porous scaffolds could be formed through corresponding freeze-drying. Interestingly, a bone mimic lamellae pore structure could be obtained by using this kind of freeze-drying process to fabricate RSF scaffold. For example, Chen et al. successfully fabricated a kind of biomimetic scaffold with strong mechanical property and bone like-lamellae pore structure via a suitable multi-staged freeze-drying method by using proper mass ratio of SF and bacterial cellulose nanofiber ribbon (BCNR) [83].

3.5. 3D printed RSF scaffold

As an additive manufacturing strategy, 3D printing, such as extrusion

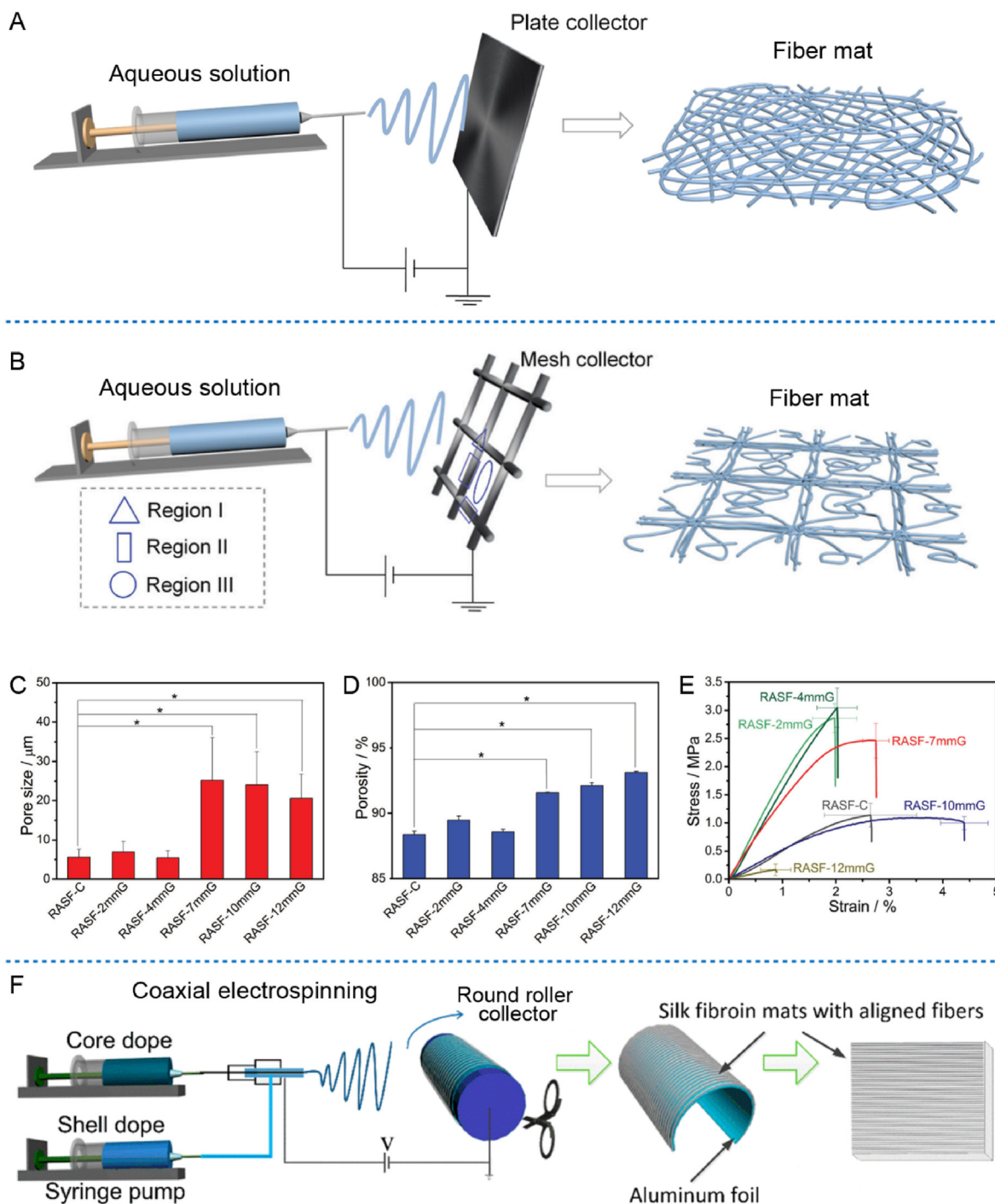


Fig. 4. Preparation of electrospun RSF fiber mats from its aqueous spinning dope. (A) Schematic illustration of the electrospinning using traditional intact plate (RASF-C) or mesh collectors with gap sizes of 2 mm (RASF-2mmG), 4 mm (RASF-4mmG), 7 mm (RASF-7mmG), 10 mm (RASF-10mmG) and 12 mm (RASF-12mmG), respectively. (D) Statistical results of the porosity of fabricated fiber mats. (E) Stress-strain curves of post-treated electrospun fiber mats. (F) Schematic presentation of the fabrication of RSF fiber mats with aligned fibers by coaxial electrospinning using round roller collector. Images (A)–(E) were modified with permission [79]. Copyright 2021, The Royal Society of Chemistry. Image (F) was modified with permission [31]. Copyright 2016, American Chemical Society.

printing and digital light processing (DLP) printing can both feasibly fabricate complex material shapes according to specific requirements, thus quite well meet the requirements of personalized medicine. It has been reported that the SF bioink exhibited the required shear thinning behavior at relative low concentrations (<20%) for printing before gelation. However, pure SF solution was difficult to form a self-standing construct with high shape fidelity [84]. In order to meet the requirements of rheology and viscosity for an effective bioink, a potential method is

blending other high viscosity biomaterials, such as gelatin, chitosan, or alginate *etc.*, to prepare hybrid bioinks [85–88].

Until now, a few kinds of SF based hybrid bioinks and corresponding 3D printed scaffolds have been developed [85]. For example, by using the glycerol for inducing physical crosslinking, Rodriguez et al. printed a series of SF/gelatin scaffolds with elastic modulus ranged about 50–1000 Pa [89], which was well within the range of soft tissues. Shi et al. further used the genipin to crosslink the SF and gelatin in the hybrid bioink,

then obtained composite 3D printing scaffolds with elastic modulus ranged about 13–17 kPa [90]. In order to meet the requirements of hard tissue, the mechanical properties of the 3D printed RSF based scaffolds need to be further improved [91]. Based on these requirements, Huang et al. tried to combine bacterial cellulose nanofibers (BCNFs) with the SF/gelatin mixed bioinks to simultaneously improve the shape fidelity and mechanical properties of printed scaffolds [91], as schematically shown in Fig. 5A. Results illustrated that the tensile strength of printed composite scaffold increased obviously (from 100 kPa to 800 kPa) with the addition of BCNFs. Expected multi-level porous structures in the scaffolds were also obtained by designing proper lyophilization after the extrusion printing [91], as shown in Fig. 5B. In addition, the incorporation of BCNFs into bioinks have also provided an ECM-like filamentous architecture aligned along the printed filaments in the scaffold.

TEMPO-mediated oxidation could provide electrostatic repulsions between micro or nanofibers including BCNFs by introducing certain amount of carboxylate groups, which facilitates the dispersion and processing of oxidized micro or nanofibers. Using SF and TEMPO oxidized bacterial cellulose nanofibers, Huang et al. further developed a simple and novel binary composite bioink [92]. In this binary bioink system, SF bulks were cross-linked by horseradish peroxidase (HRP)/H₂O₂ to form printed hydrogel scaffolds. Proper mass ratio of the oxidized bacterial

cellulose nanofibers promoted the viscosity of the inks and further improved the mechanical properties and shape fidelity of the scaffolds. Moreover, the nanofibers could also be induced to align along the printed filaments. Besides the mentioned gelatin and BCNFs being applied as additive component, the printability of SF based bioinks could also be improved with alginate [93].

Another useful strategy is using chemical modification to prepare demanded silk fibroin based bioinks. For example, Kim et al. have successfully developed a chemical modified SF based bioink for DLP 3D bioprinting [86], as presented in Fig. 5C. More specifically, through the amino groups (-NH₂) on the SF segments, the SF is covalently immobilized with glycidyl methacrylate (GMA), which is a donor of vinyl double bond as a UV-crosslinking site, as schematically shown in Fig. 5D. Then the lithium phenyl(2,4,6-trimethylbenzoyl) phosphinate (LAP) was added to GMA-modified SF solution to form a novel photopolymerizable Sil-MA biolink [86]. It has been reported that this kind of Sil-MA hydrogel showed an excellent mechanical and rheological properties. And the outstanding printability and printing accuracy of the 30%Sil-MA bioink have allowed scientists to successfully build the organ mode with highly complex morphologies and structures, including the brain, ear, trachea, heart and lung *etc.* [86], as partially shown in Fig. 5E. This kind of researches provided an effective chemical modification strategy for the

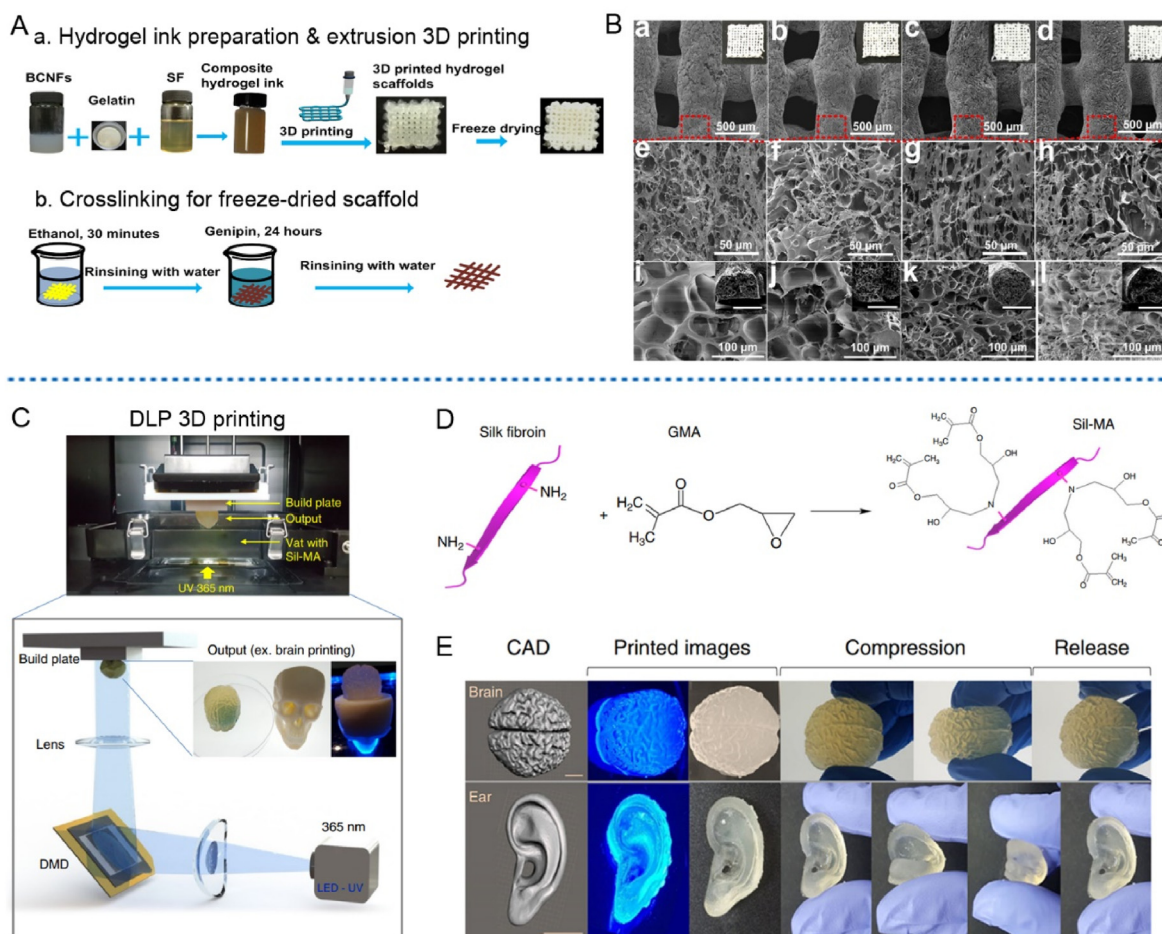


Fig. 5. Fabrication of SF based bioinks and corresponding printability evaluation by using extrusion or DLP printers. (A) Schematic illustration of the processing route for preparing SF/gelatin/BCNFs hydrogel bioink and corresponding 3D printed scaffold. (B) SEM images of (a, e, i) BCNFs-0 wt%, (b, f, j) BCNFs-0.35 wt%, (c, g, k) BCNFs-0.70 wt%, (d, h, l) BCNFs-1.40 wt% scaffolds to show the hierarchical structure of the printed scaffolds. (a–h) Surface observation of printed scaffolds. (i–l) Cross section of printed filaments (inserted scale bars: 500 μ m). (C) Schematic presentation of the DLP bioprinting procedure using DLP printer and Sil-MA bioink. DMD was the digital micromirror device. (D) Schematic illustration of the chemical modification of SF molecule with GMA to fabricate Sil-MA bioink. Herein, GMA is a donor of vinyl double bond as a UV-crosslinking site. (E) CAD models and corresponding gross views of the 3D printed brain and ear shape mimicked RSF scaffolds. Scale bar indicates 1 cm. Images (A)–(B) were modified with permission [91]. Copyright 2019, Elsevier Ltd. Images (C)–(E) were modified with permission [86]. Copyright 2018, Springer Nature.

fabrication of SF based bioinks and suggested that the photopolymerizable Sil-MA bioink would be an excellent alternative for DLP printing of RSF scaffold.

3.6. RSF hydrogel

RSF hydrogel could be constructed either by physical crosslinking or chemical crosslinking. As for the physical crosslinking in biomedical applications, it was commonly used a mild physical stimulation as trigger, such as ultrasonic stimulation [94]. Specifically, SF solution need to be prepared at first and then formed a transparent and fluid phase with a short ultrasonic stimulation at relatively low power. This state is the intermediate state of solution to gel transition. After being incubated in a cell incubator, corresponding physical crosslinking hydrogel could be easily formed mainly through the formation of β -sheet structure as physical crosslinking sites (see Fig. 6A). Other methods such as electrical stimulation and vortex oscillation induced physical crosslinking strategies have also been used to fabricate RSF hydrogel [2].

RSF hydrogel could also be feasibly constructed with a mild chemical crosslinking mechanism. The proposed scheme usually relies on the formation of di-tyrosine bond between tyrosines in the SF molecule [95–98]. Corresponding formation mechanism is briefly illustrated in Fig. 6B. The selection of mild reaction system is made sure that the living cells can be wrapped smoothly for culture and further investigation. Just for this consideration, two mild methods are usually applied as follows. (1) Thermal-induced crosslinking system [99]: it needed to mix the SF solution, horseradish peroxidase (HRP) solution and hydrogen peroxide (H_2O_2) solution in a proper ratio, then incubated the mixture in a thermostatic equipment, such as cell incubator at 37 °C to form cross-linked hydrogel. (2) Visible light induced crosslinking system [96]: SF aqueous solution with appropriate concentration, tris (2,2-bipyridyl) dichloro-uthenium (II) hexahydrate (Ru) solution and sodium persulfate (SPS) solution were firstly mixed at an appropriate proportion and then

initiated by a visible light source. In addition, the riboflavin has also been reported as an effective enzyme catalysis to form di-tyrosine bond based RSF hydrogel [100]. Except for the described mechanism of di-tyrosine bond formation between tyrosines, some other chemical modification strategies to the silk fibrin molecule, such as methacryloyl-modification by immobilization of vinyl double bond as a sensitive crosslinking site has also been applied to form chemical crossing RSF hydrogel [86,101].

Herein, the detailedly mentioned physical and chemical crosslinking strategies are quite suitable for active growth factor or even live cells loading, thus much suitable for cell culture and tissue engineering. In order to realize related applications, it just needs to add corresponding live cells, growth factors or active drugs into the mixed solution just before the initiation of the physical or chemical crosslinking.

3.7. Patterned RSF substrate

SF molecule can be extracted into aqueous solution, which is very beneficial for the preparation of various RSF biomaterials. Among them, the patterned RSF substrates with regular micro or nanofeatures were commonly used to regulate cell behaviors, deeply reveal corresponding cell-material interactions, or even used as flexible bioelectrode. Generally, the patterned RSF substrates could be fabricated by cast molding [69,102], etching [103], or printing technologies [104,105]. And the pattern features could be effectively regulated by the mold design and related material engineering processes.

As for the cast molding, the SF solution was pretreated to remove residual bubbles. An appropriate volume of SF solution was then cast into the pre-prepared mold with inverted topological features. Following that, the mold was covered with a venting lid and allowed to air dry at room temperature [102]. The substrate thickness could be regulated by adjusting the ratio between the volume of SF solution and the bottom area of mold. The RSF substrates were then peeled from the mold after drying and then immersed in ethanol or incubated in a high humidity

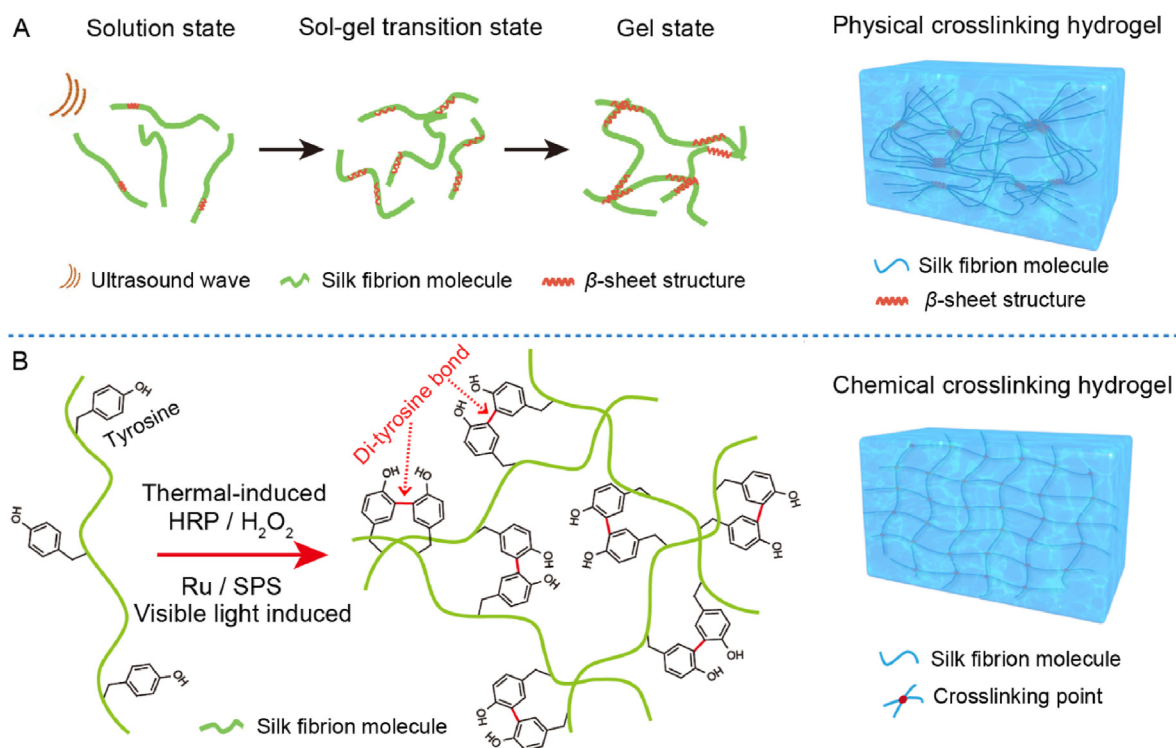


Fig. 6. Formation of RSF hydrogel through mild physical or chemical crosslinking. (A) Schematic illustration of the formation mechanism of physical crosslinking hydrogel induced by ultrasonic stimulation. (B) Schematic illustration of the formation mechanism of chemical crosslinking hydrogel induced by thermal or visible light stimulations.

environment to create water-insoluble substrate. Finally, the inverted topological patterns on the mold could be successfully transferred onto the RSF substrate, as briefly illustrated in Fig. 7A.

There is also a growing interest in material surface patterning by direct etching or writing *via* tailored energy exposure [68,103]. Polymer material such as RSF substrate could be directly etched by high-energy laser, ion, or electron beam, as schematically shown in Fig. 7B. Through the programmed scanning of the high-energy beam, designed topological patterns can be feasibly fabricated onto the surface of RSF substrate. In the direct laser ablation of relative thick RSF film, it was reported that the ultra-short femtosecond laser pulses at near-IR wavelength could make the high precision laser cutting (or etching) achievable, while direct absorption of UV photons could usually give rise to 3D foams with large surface area [106].

Interestingly, it was demonstrated that SF aqueous solution could be directly used as a positive or negative photoresist [107,108] in the electron beam lithography (EBL). Firstly, a spin-coated RSF film on the substrate was prepared. For positive resist work, the RSF film was then crosslinked or crystallized by alcohol treatment. After high energy electron beam exposure, the crosslinked region in the expose region could be de-crosslinked and the β -sheet network in these regions will be unzipped. Corresponding effect will finally inducing the exposed regions water-soluble [107,108], as schematically presented in the upper row of

Fig. 7C. For negative resist work, the spin coated RSF film was then directly exposed by low energy electron beam exposure, the expose regions could be crosslinked under electron beam exposure. Corresponding effect could finally induce the exposed regions water-insoluble [107, 108], see the lower row of Fig. 7C. So, after electron beam exposure and water development, a “photolithography” caused RSF patters could be fabricated on the substrate.

Another commonly used pattern formation technique is printing, which could successfully generate chemical patterns on the RSF substrate. For example, inkjet printing is a non-contact, cost effective, highly controllable and time saving strategy that can print designed patterns (via software design) onto the RSF substrates [105], see Fig. 7D. The advantage of inkjet printing is its ability to precisely print pico-litres of ink at predesigned locations either side by side, or one on other top, inducing diverse patterns with chemical contrast [105]. Moreover, with the development of multiple print head and corresponding controlling technologies, it also enables fast and personalized fabrication at large scale. In inkjet printing on the RSF substrate for biomedical applications, a few kinds of biocompatible materials such as fibronectin, poly-L-lysine, collagen, special peptide sequences (such as IKVAV, YIGSR and RGD), or conductive gold and silver were generally used as bioinks to print desired chemical patterns or circuit diagram on the RSF substrate [104], as schematically illustrated in Fig. 7D.

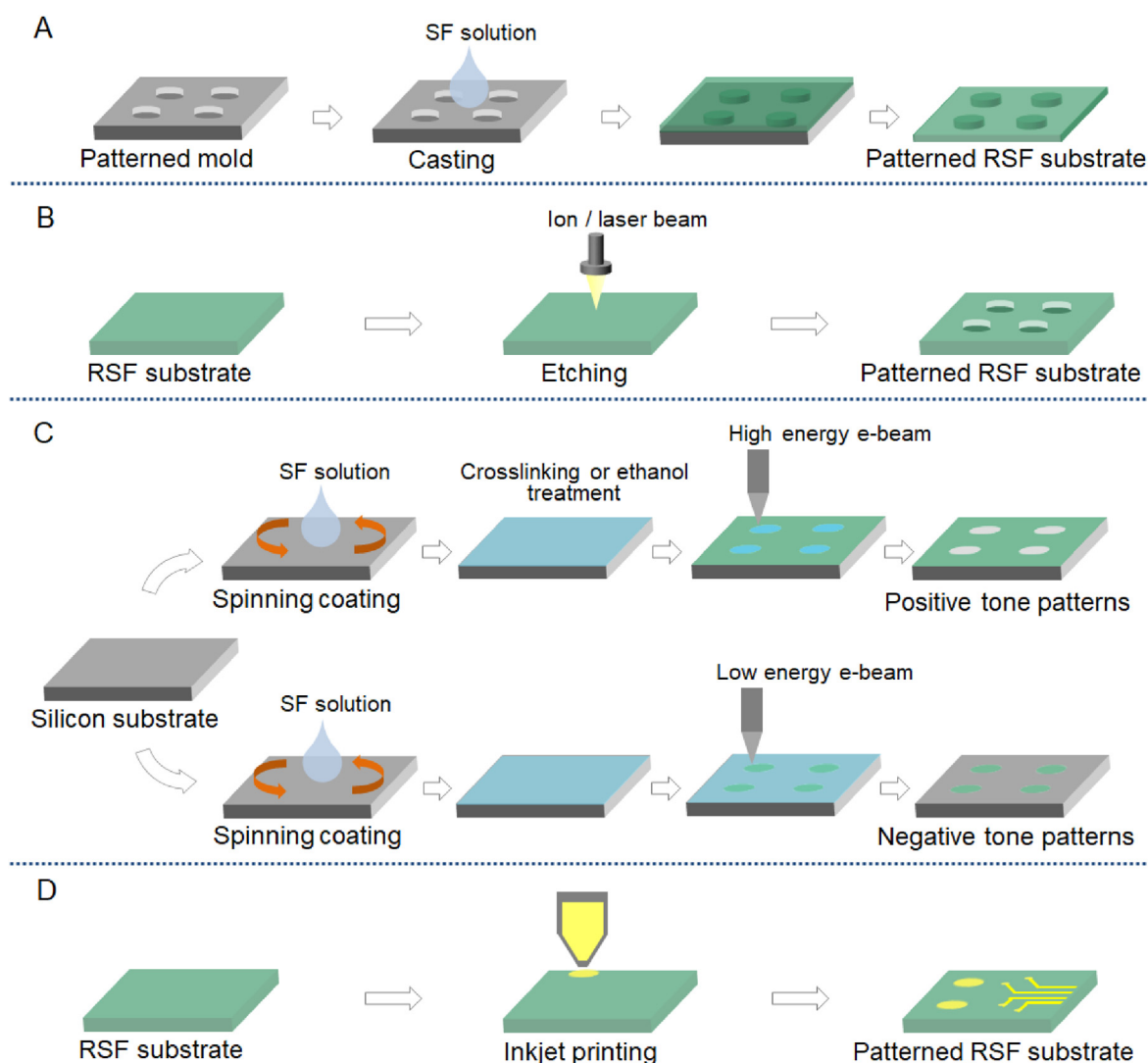


Fig. 7. Schematical presentation of the typical fabrication strategies to prepare patterned RSF substrate. (A) Cast molding. (B) Direct etching. (C) Electron beam lithography using SF solution as positive or negative photoresist. (D) Inkjet printing.

4. Advanced biomedical applications of RSF materials

Until now, as the remarkable biocompatibility, excellent mechanical properties, tailorable biodegradability, sufficient supply, and excellent processibility, the RSF material has been widely used in biomedical applications. In this review, we are more focused on its unique application in the fields of cell-material interactions, soft tissue engineering, and flexible bioelectronic devices. As for the other important biomedical applications, such as wound dressing, hard tissue engineering and drug delivery *etc.*, extensive descriptions could be seen from previous publications [28,29,109–117].

4.1. Cell-material interactions

From the solution or suspension of the extracted building blocks, RSF biomaterials with desired topological, stiffness, or chemical contrast features in 2D film or 3D scaffold could be feasibly constructed, and hence provided a powerful material platform for the study of cell-material interactions. This kind of study is quite important for understanding different material cues effect on cell behaviors, thus much valuable for the design, fabrication, and modification of effective biomaterials [118–123]. Based on the developed material fabrication and surface patterning technologies, some valuable cell-material interactions have been revealed via the RSF materials, which will be comprehensively summarized as follows.

4.1.1. Effect of micro or nanogrooves on cell behaviors

Modifying RSF materials with proper topological features is a feasible way to regulate cell behaviors. In this research field, Gil et al. have fabricated grooved RSF film with varied depth (37–342 nm) and width (445–3582 nm), then carefully evaluated fibroblast cell adhesion on these grooved surfaces. It indicated that deeper surface grooves increased cellular alignment along the direction of the groove features (as usually called cell contact guidance) [124]. Based on this exploration, Tien et al. further fabricated grooved RSF film with 515 nm in depth and 3597 nm in width, then evaluated corresponding cell adhesion and differentiation behaviors on the grooved or flat films [19]. Results indicated that grooved RSF film not only enhanced the osteogenic differentiation of MSCs, but also produced robust alignment of cells and cortical bone specific ECM along with groove direction. More interestingly, a subsequent layer of cells grows at a rotated angle of alignment from the initial layer (aligned along groove direction) during the following cell osteogenic differentiation process, while only random cell direction was observed on the flat films [19]. The mentioned initial contact guidance of the bottom cell layer and subsequent realignment effect of the upper cell layer observed on the groove patterned RSF films raised the possibility that simple topographical features might be applied for inducing more complex, high ordered 3D tissue structures.

Recently, according to the natural tendon structure. Lu et al. fabricated a bionic grooved RSF film, and set flat RSF film as control [125]. The grooved RSF film presented parallel grooves that were 10 μm in width, 5 μm in depth, and 10 μm between adjacent grooves, as shown in Fig. 8A. Through carefully investigation of the tendon stem/progenitor cells (TSPCs) adhesion, tendon differentiation and focal adhesion kinase (FAK) activation response on the flat and grooved surfaces, it indicated that the RSF films with this microgroove feature could induce TSPCs to be an oriented alignment with slender morphology along with the underneath micro grooves, as presented in the third column of Fig. 8A. As for the tendon differentiation, the expression of tenogenic genes and secretion of proteins, such as scleraxis (SCX), tenascin-C (TNC), tenomodulin (TNMD), collagen type I alpha chain (COL1A1), and activated FAK (pFAK, phosphorylated focal adhesion kinase) were evaluated and higher expression were found on the grooved surface. In addition, the FAK inhibitors blocked the enhanced expression of tenogenic genes and proteins, corresponding western blot analysis of the protein expression was shown in Fig. 8B. So, the grooved surface also significantly enhanced the

stem cell tendon differentiation by activating the FAK phosphorylation [125].

Through the fabrication of RSF films with a variety of surface patterns, such as square wells, square pillars, round wells plus square pillars, and grooves (356–880 nm in width), Du et al. also carefully evaluated human umbilical vein endothelial cell's (HUVEC) response on related topological features [126]. Among them, cell contact guidance effects have been significantly observed on groove patterns, while on the smallest topographic surface containing groove features, the cells presented a decrease in orientation and alignment. Moreover, for crossing the grooves, it found that filopodia altered their primary growth orientation on the ridges to choose the shortest pathway on different patterns. In addition, when compare to the flat RSF film, cell proliferation were enhanced on the square wells and grooves with largest features, while inhibited on the square pillars and grooves with smallest topographic features [126]. The microgroove patterned RSF films have also been proved to significantly induce contact guidance for endothelial cell, smooth muscle cell, and fibroblast cell by Gupta et al. [127]. These reports would be useful to understand the importance of incorporating varied groove features within material surface to regulate cell behaviors and provide valuable reference for the construction of effective RSF bioscaffolds, especially in the field of nerve, tendon, muscle and blood tissue repairing.

4.1.2. Effect of microconvex dots or micropillars on cell behaviors

The microscale convex dots or pillars on the RSF materials have also been proved to have significant effect on cell behaviors. For example, Tang et al. fabricated microconvex dots featured RSF films with the density ranging from 37 to 4835 dots/ mm^2 [128], as schematically illustrated in Fig. 8C. It indicated that the cells presented spindle shapes on the surface with lower convex dots density and satellite shapes on the surface with higher density. Interestingly, modified RSF film with proper density about 2899 convex dots/ mm^2 not only boosted adhesion, spreading, and proliferation of HUVECs, but also promote corresponding angiogenesis, as schematically summarized in Fig. 8C. Moreover, this regulated gene expression process was proved to be associated with cell shape-regulated Yes-associated protein (YAP) activation. *In vivo* mouse subcutaneous implantation of the films also confirmed the angiogenesis enhancing effect of this proper convex dot-featured RSF film [128]. This study offered an effective method in angiogenesis-promotable material modification in tissue engineering. In addition, using polystyrene microsphere self-assembling, microsphere shaped convex (with fixed diameter about 7 μm) patterns were fabricated on RSF films by You et al. [130]. Then corresponding cell-material interactions were investigated by culturing rBMSCs on the RSF films [130]. It founded that just after cell seeding, the filopodia sensed and anchored to the microsphere shaped convex to form initial attachments, the anchored filopodia then converted into lamellipodia, and this conversion initiated the directional formation of lamellipodia and finally determined corresponding cell spreading. Further evaluation revealed that this topological features modified films enhanced cell adhesion and proliferation due to promoted lamellipodia formation, with recognition and conversion of filopodia into lamellipodia as a critical role in cell response to this kind of convex features [130].

Interestingly, different responses between normal cell and pre-cancer cell have also been reported on a suitable micropillar featured RSF film [131]. Specifically, by using replication process from the natural lotus leaf template, Rajput et al. fabricated RSF based films with varied micropillar structures and reported a differential proliferation behavior of normal and fibrosis associated human oral fibroblasts (pre-cancer cell) on micropillar featured honey embedded RSF substrates [131]. Comparison illustrated that the proliferation rate is maximized for normal fibroblast, while it obviously inhibited for fibrosis associated fibroblasts on the micropillar surface with moderate height of about 8.5 μm and 2% honey concentration [131]. This study provided a valuable insight into the cancer therapeutic strategies for preventing pre-cancer progression

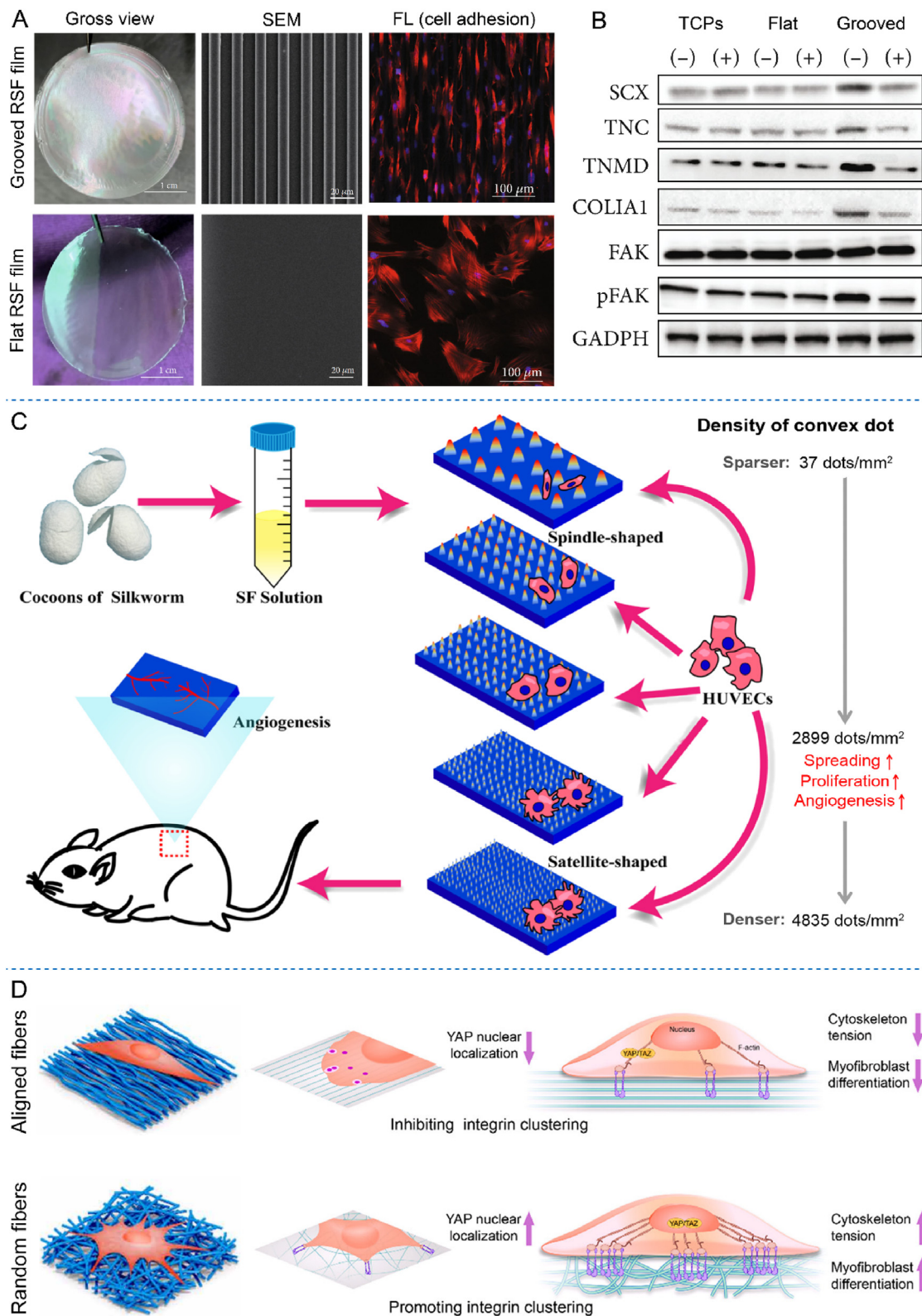


Fig. 8. Effects of varied RSF material cues on cell behaviors. (A) The topological features and tendon stem/progenitor cell adhesion behaviors on the fabricated grooved RSF film and flat RSF film. SEM: scanning electron microscope, FL: fluorescence microscope. (B) Western blot results of the protein expression of SCX, TNC, TNMD, COLIA1, FAK, pFAK and GAPDH. TCPs: tissue culture plates, (-): without FAK inhibitor, (+): with FAK inhibitor. (C) Schematic illustration of the fabricated RSF films with different microconvex dot densities, and its effects on HUVECs adhesion, proliferation, and angiogenesis, which were evaluated both *in vitro* and *in vivo*. (D) Schematic illustration of the effect of SF/Col-I fiber arrangement on fibroblasts behaviors. Images (A)–(B) were modified with permission [125]. Copyright 2020, Hindawi Ltd. Image (C) was modified with permission [128]. Copyright 2021, American Chemical Society. Image (D) was modified with permission [129]. Copyright 2020, American Association for the Advancement of Science.

toward cancer through discriminating cell response to the special topological featured substrate.

4.1.3. Effect of fiber arrangement on cell behaviors

The comparison of cell responses to the aligned and random fiber arrangement is also an important topic in cell-material interactions and has been widely studied in the scientific community. For example, Madduri et al. fabricated special nerve conduits topographically functionalized with aligned or random RSF nanofibers [20]. Cell adhesion results illustrated that dorsal root ganglions sensory neurons and spinal cord motor neurons both exhibited an elongated cell length and axonal outgrowth along with the aligned RSF nanofibers. In contrast, the growth direction of axonal and glial presented randomly, and corresponding length was also much smaller on the random RSF nanofiber distributed surface [20]. This study provided useful guidance for the construction of artificial nerve conduits, which can be used for enhance the repair of small nerve gaps.

Moreover, Xu et al. further reported that aligned RSF based fiber features could not only induce the elongation and bipolarization of fibroblasts, but also suppressed fibroblasts to myofibroblast transition by inhibiting integrin clustering and reducing cytoskeleton tension [129]. While the random distributed fibers promoted the myofibroblast differentiation by promoting integrin clustering and increasing cell tension, as schematically summarized in Fig. 8D. Furthermore, YAP molecule signaling activities regulated by this kind of special topological cues has also been verified [129]. By using the untraditional mesh collector with varied gap sizes, Zou et al. firstly attempted to fabricate a kind of novel electrospun RASF mats with hierarchical structures and improved mechanical properties [79]. Interestingly, relative aligned fibers were well collected on region II (near the non-cross-point zone of metal wires) and random distributed fibers were collected on region I (near the cross-point zone of metal wires) of the mesh collector. So, aligned or random distributed RSF fibers have been fabricated on the same microregion of the fiber mat. Schwann cells in region II of the fiber mat demonstrated elongated morphology along with corresponding fibers, while cells could only present spherical morphology on the regions (region I) with randomly oriented fibers. These studies about the cell responses on the fiber mats with controllable arrangement have inspired a novel and feasible way to modify related biomaterials.

4.1.4. Effect of pore size of the scaffold on cell behaviors

Porous RSF scaffolds have been widely used for tissue repair and regeneration. In order to elucidate the pore size features effect on cell behaviors, Ai et al. constructed series of RSF scaffolds with average pore size (diameters) of about 174 μm , 275 μm , and 384 μm by using salt leaching method, which were denoted as small, medium, and large groups [21], as illustrated in the first row of Fig. 9. Then, porcine BMSCs were seeded on these scaffolds and cultured for 21 days in osteogenic medium to evaluate the pore size effect on cell proliferation and osteogenesis. It indicated that scaffolds with smaller pore sizes showed beneficial for cell proliferation and osteogenic differentiation compared to the excessive pore sizes (275 μm and 384 μm), which is evidenced by higher cell metabolic rate, more cells numbers and higher expression of osteogenic biomarkers [21], as partially shown in the second and third rows of Fig. 9. In summary, it founded that the RSF scaffolds with an appropriate pore diameter of about 174 μm was optimal for cell proliferation and osteogenic differentiation of BMSC.

As for the electrospinning scaffold, the pore size of the scaffold has also been proved to have profound effect on cell behaviors. By combining multi-step electrospinning with low temperature (LTE) collecting, Huang et al. have fabricated a special RSF electrospun scaffolds with gradient pore size [132]. Results illustrated that traditional electrospun scaffolds with small pore size (average diameter about 6 μm) restrained cell (L929 cell) proliferation and infiltration into the scaffold when compare the

scaffold with larger pore size. On the contrary, LTE electrospun scaffolds with medium pore size (about 12 μm) significantly enhanced cell proliferation. Relative large pore size scaffolds (about 37 μm) was beneficial for cell growth and especially favored for cell infiltration into the inner scaffolds [132]. In addition, Zou et al. also reported that the electrospun RSF scaffold with higher pore sizes presented relatively higher cell viability, better cell proliferation, deeper cell permeation, and even faster cell migration of Schwann cells than those with smaller pore sizes. These studies have highlighted the importance of pore size features of the RSF scaffold in biomedical applications and might provide universal references for regulating the performance of other porous scaffolds.

4.1.5. Effect of substrate mechanical properties on cell behaviors

Mechanical properties, such as stiffness and elastic modulus of the RSF matrix has also been proved as important factors to influence cell behaviors. For example, Edwin et al. have prepared RSF hydrogels with varied stiffness from 0.7 kPa to 3.1 kPa. Subsequently, NIH3T3 fibroblast cells were cultured on the surface of corresponding hydrogel. It has been reported that the increase of hydrogel stiffness decreased nucleus-to-cytoplasm area-ratio and increased asymmetricity along the major-axis of cells [22]. Moreover, using traction force microscopy (TFM), they have carefully quantified corresponding cell traction stress on the hydrogel surface. Cells plated on relative stiff hydrogel (3.1 kPa) exhibited significantly higher traction stress as compared to that on soft ones (0.7 kPa). All together, these results hinted that the stiffness of RSF substrate could significantly regulate cell adhesion and cell traction stress. More interestingly, the cell differentiation, such as osteogenesis of BMSCs has also been proved to be significantly regulated by the stiffness of RSF substrate. In this topic, Long et al. have fabricated three kinds of RSF substrates with high, medium, and low stiffness by varying the β -sheet content [133], which were named as SFH, SFM, and SFL groups respectively, as shown in Fig. 10A–B. Except for the stiffness, the substrates presented similar chemical composition, surface topography, and wettability. When adsorbed fibronectin, the stability of the adsorbed protein-material interface increased with the increasing of stiffness of the RSF substrates. Finally, larger areas of cytoskeleton-associated focal adhesions, higher orders of cytoskeletal organization and more elongated cell spreading were all observed for BMSCs cultured on RSF substrates with high stiffness than lower ones, along with enhanced nuclear translocation and activation of YAP/TAZ [133]. The stiff RSF substrate with higher β -sheet content further enhanced the osteogenesis of BMSCs, evidenced by higher expression of ALP and collagen I, and also denser deposition of calcium [133], as presented in Fig. 10C–H.

The elastic modulus effect of RSF substrate on cell behaviors have been reported by Amirikia et al. [134]. In this study, series of RSF porous scaffolds were prepared by freeze drying through SF solution with varied concentrations. The produced scaffolds presented minimal changes in the pore size but with elastic modulus from 16 to 131 kPa in the wet condition [134]. Then, apical papilla stem cells were choosing to evaluate cell adhesion and osteogenesis. Results illustrated an increased osteogenic differentiation along with the increasing of the modulus from 16 kPa to 83 kPa, and then a sudden decrease of osteogenic differentiation was observed in the scaffold with modulus about 131 kPa [134]. These researches clearly illustrated the mechanical properties of the RSF substrate could significantly affect cell adhesion and differentiation, which could provide useful references for the design of effective scaffold and cell culture substrate used for biomedical applications.

4.1.6. Effect of chemical modifications on cell behaviors

The chemical modification of RSF material is a useful and powerful way to regulate cell behaviors and hence could enhance the biofunction of RSF biomaterials. As for these research topics, Wang et al. have successfully fabricated polydopamine (PDA) modified RSF film and evaluate corresponding cell responses [24]. It founded that the PDA coating

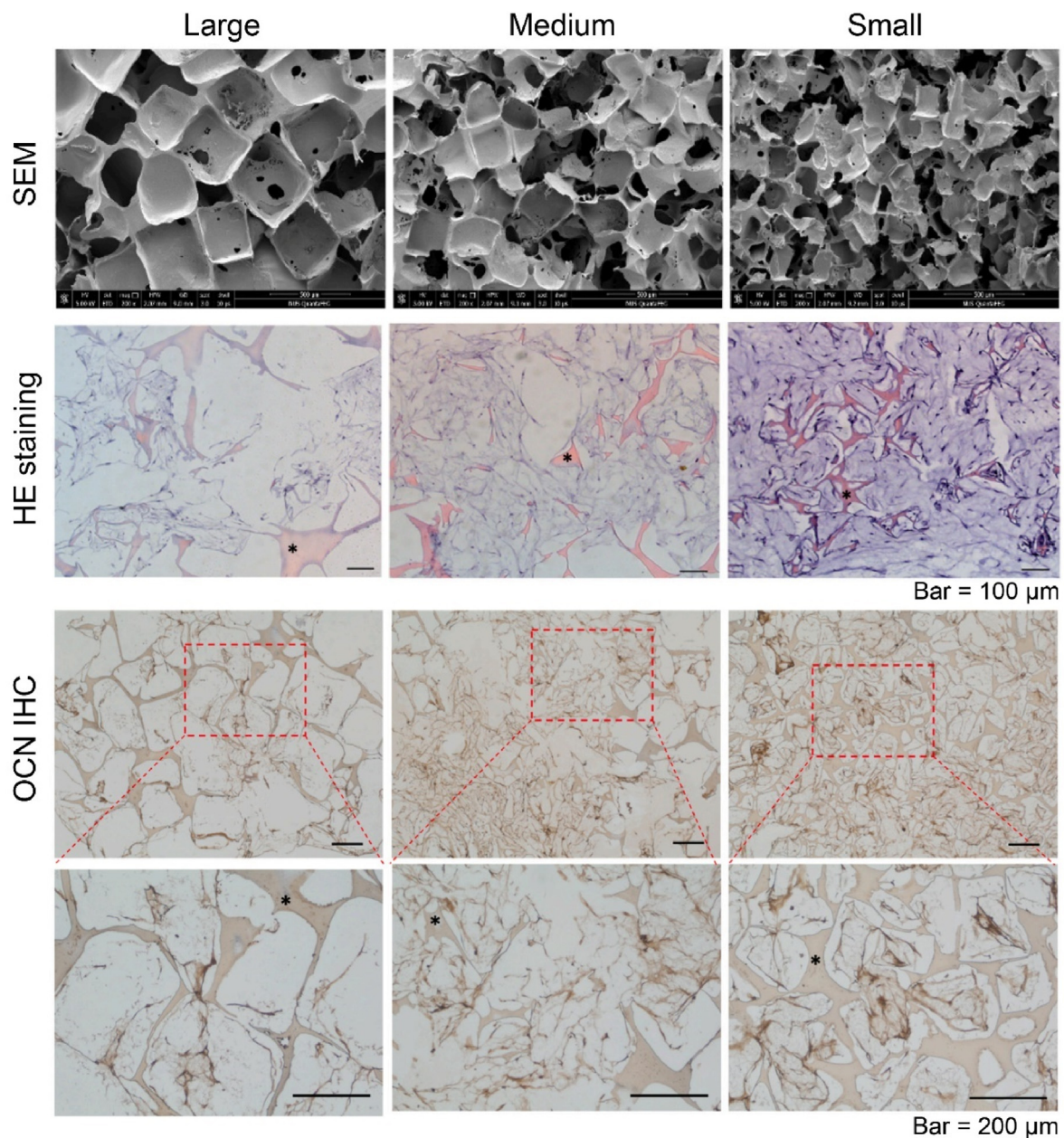


Fig. 9. Effect of pore size of the RSF scaffold on BMSC behaviors. The first row is the SEM photographs of RSF scaffolds with large, medium, and small pore sizes. The second row is the HE staining of BMSCs on corresponding scaffolds after 21-day osteogenic differentiation. The third row is the immunohistochemistry (IHC) staining of OCN (one of the osteogenic biomarkers) after 21-day osteogenic differentiation. Asterisks indicate RSF scaffolds. Reproduced with permission [21]. Copyright 2021, Elsevier B.V.

obviously increased the roughness and hydrophilicity of the film surface and thus enhanced its protein absorption capability. Furthermore, the PDA modified films significantly promoted the adhesion and migration of MSCs in the *in vitro* wound healing model [24]. Besides, laminin-coated SF based electrospun fiber mats have also been investigated and proved to enhance the neural progenitor cells proliferation and neural differentiation [135].

In general, by decorating with integrin-binding peptide motifs is another effective way to enhance the biofunction of RSF materials. For example, by decorating RSF films with YIGSR and GYIGSR, Manchineella et al. have investigated its effect on hMSCs behaviors [17]. Intriguingly, covalently functionalized RSF film with the hexapeptide of GYIGSR enhanced hMSCs proliferation and neuron differentiation when compared with YIGSR modified surface and untreated RSF surface. The improved neuron differentiation were confirmed by the higher

expression of neuronal-specific genes, such as MAP2, TUBB3, and NEFL [17]. This kind of chemical modification attempts further enhanced the potential of RSF based materials for neural therapy applications. In addition, Wei et al. also investigated the effects of RGD and stem cell factor (SCF) modified RSF scaffold on the behaviors of apical papilla stem cells based on the construction of RSF, RSF-RGD, RSF-SCF, and RSF-RGD-SCF scaffolds [136]. It has demonstrated that when compare to other modification strategies, the RSF-RGD-SCF composite showed optimal promotion for the adhesion, migration, and proliferation of apical papilla stem cells, making it a promising candidate for cell-homing pulp regeneration [136].

Chemical modification is a feasible and effective strategy to regulate corresponding cell behaviors. The above mentioned attempts have provided valuable reference for the effective modification of SF based bio-materials, which are hopefully to be used for accelerating specific cell

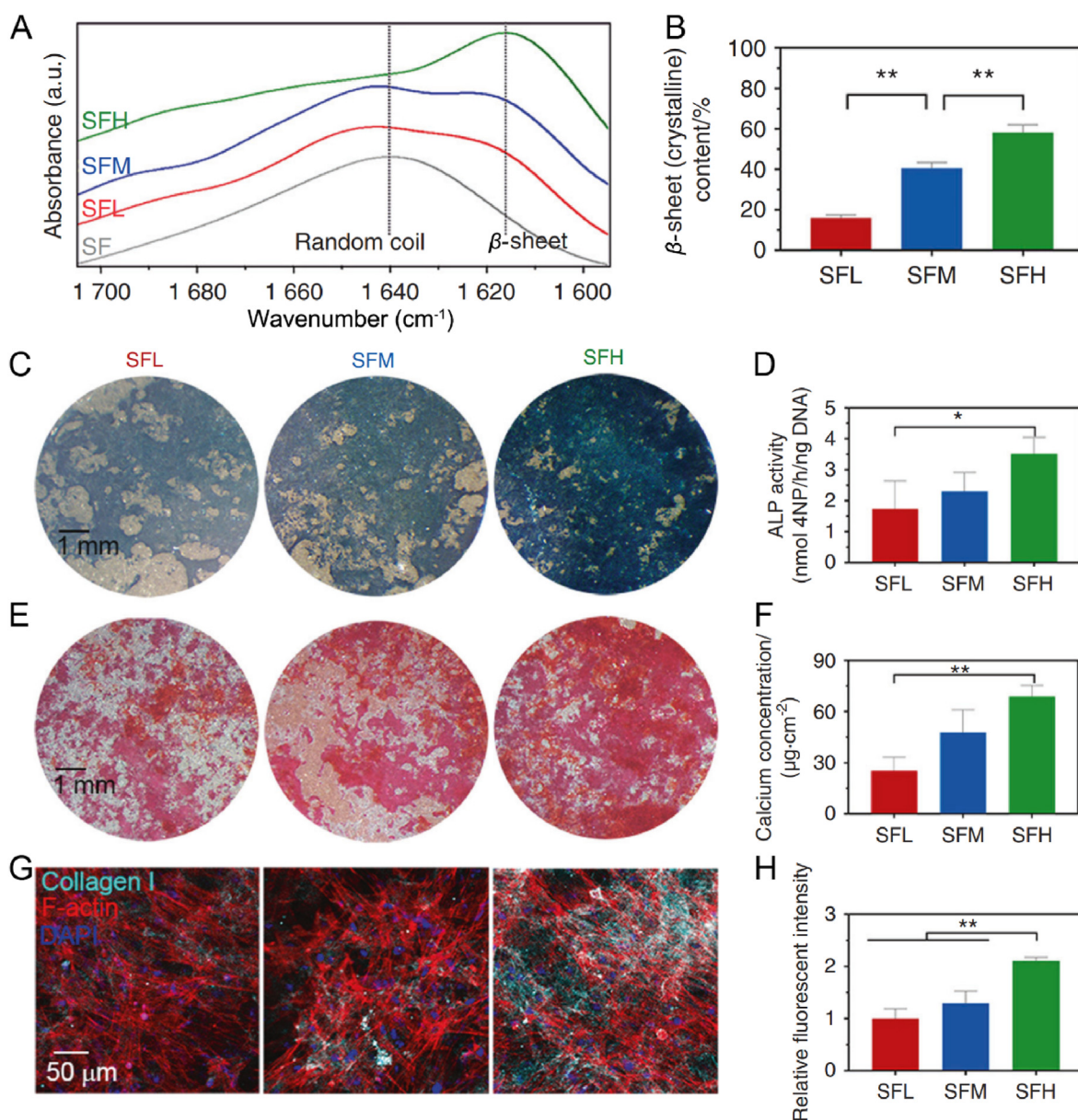


Fig. 10. Effect of substrate stiffness on BMSCs osteogenesis. (A) FTIR results of the amide I region obtained from the fabricated RSF substrates. (B) Calculated β -sheet contents by Fourier self-deconvolution from figure (A). (C) Images of ALP staining in BMSCs at day 7. (D) Quantitative detection of ALP activity in BMSCs at day 7. (E) Images of ARS (Alizarin Red S) staining in BMSCs at day 14. (F) Quantitative analysis of calcium deposition in BMSCs at day 14. (G) Immunofluorescence images of collagen I and F-actin staining in BMSCs at day 14. (H) Quantitative analysis of fluorescence intensity of collagen I in BMSCs at day 14. The RSF substrate with high, medium, and low contents of β -sheets were denoted as SFH, SFM, and SFL group, respectively. Reproduced with permission [133]. Copyright 2021, Springer Nature.

growth and tissue regeneration.

4.2. Soft tissue regeneration

Be different from the limited processibility of natural silk, varied formats of RSF biomaterials with different properties can be easily fabricated based on these extracted building blocks. Combined with the excellent biocompatibility and adjustable biodegradability, the RSF material can be used for effective tissue repair in a wide range of tissues and organs. In this section, we are more focused on the typical applications of RSF biomaterials in tissue regeneration of soft tissues, especially for the urethral, nerve, and liver. For more information about the regeneration of intensely reported hard tissues, some relevant literatures are recommended [4,28,137,138].

4.2.1. Urethral regeneration

Urethral stricture is the commonly pathogenesis of lower urinary tract symptoms in human. The strictures in distal location along the penile shaft or relative long strictures (larger than 2.5 cm) often require urethra reconstruction, which need to use related substitutive materials to augment and repair the stenotic segment [139]. To screening suitable substitutive material used for the urethral strictures repair becomes one of the most challenging topics. Until now, many scientists have tried to develop suitable biodegradable materials for urethral reconstructions. A few kinds of natural matrices, including bladder acellular matrix (BAM) [140,141] and small intestinal submucosa (SIS) [142,143], as well as popular synthetic polymeric materials were used to treat urethra stricture in preclinical or clinical stages. It has been reported that the BAM and SIS from other species or individuals may present a potential risk of disease transmission, and the acidic degradation products from most synthetic polymer probably have some negative effect for cell growth and immune

response. So, the ideal candidate material for use in urethral reconstruction remains controversial.

Electrospun RSF fiber mat may be an appropriate material for urethra reconstruction because it can create a porous scaffold in a conformation that well mimics the component and geometric features of the native ECM. Collaborated by Zhang and Xu et al. [139], they have developed a novel electrospun RSF fiber mat that were stretched in 90 vol% ethanol after electrospinning and then evaluated the application of the stretched electrospun silk fibroin matrices (SESFMs) for urethral reconstruction in a dog model. It indicated that post-operation of stretch has substantially increased the mechanical strength of the SESFMs. Then, canine urothelial cells were cultured onto the material to obtain a tissue-engineered mucosa. Results showed that dogs implanted with tissue-engineered mucosa showed no voiding difficult. Retrograde urethrography illustrated no evidence of stricture and corresponding histologic staining presented gradual epithelial cell development and finally formed stratified epithelial layers on the surface of urethra lumen after 6 months [139], as shown in Fig. 11A–C. As for the control group (no substitute was used), the dogs showed difficulty in voiding, and histologic staining showed that no obvious epithelial cells developed during the repairing process, as shown in Fig. 11C [139,144]. Furthermore, by seeding autologous oral keratinocytes and autologous fibroblasts onto the SF based electrospun matrices, the same cooperation union successfully constructed a tissue-engineered buccal mucosa (TEBM). Then, the feasibility of TEBM in urethral defect repairing in a canine model was evaluated [145]. Results indicated that the canines implanted with the TEBM obtained effective reparation. The retrograde urethrography performed no evidence of stricture and corresponding immunohistochemical staining also illustrated that excellent epithelial layers were feasibly developed after 6 months repair under the assistance of the constructed TEBM [145]. Together, these studies confirmed that the constructed tissue-engineered grafts based on electrospun RSF matrices could serve as promising alternative scaffolds for urethra reconstruction.

In addition, rapid angiogenesis is quite important for the effective urethral repair. Generally, under the implant microenvironment of hypoxia condition, the inflammatory wound-healing response will induce the endogenous release of angiogenic growth factors, which themselves trigger the ingrowth of new blood vessels from surrounding host tissue into the implanted scaffold [146]. However, this kind of vascularization is too slow under normal condition. Because of the unique structures, the omentum is rich for vascular networks and blood supply and hence more favorable for corresponding vascularization. Recently, collaborated by Huang et al., Zhang's group [147] fabricated a few kinds of SF based composite scaffolds to evaluate their angiogenesis and urethral repair function. In this report, a few bilayer scaffolds, such as bladder acellular matrix hydrogel/electrospun RSF (BAMH/RSF) scaffold, collagen I hydrogel/electrospun RSF (CH/RSF) scaffold, and bare electrospun RSF scaffolds were fabricated. The scaffolds were firstly incubated in rabbit omentum for prevascularization and then harvested for repairing autologous urethral defects in a rabbit model. Higher levels of vascularization were formed inside the prevascularized BAMH/RSF compared with prevascularized CH/RSF and bare RSF scaffolds. The prevascularized BAMH/RSF further improved urethral tissue regeneration, which exhibited wide calibers at 3 months after implantation [147]. In addition, by using SF, 2-hydroxypropyltrimethyl ammonium chloride chitosan, and bladder acellular matrix graft through blend and coaxial electrospinning, Fan et al. further developed a kind of SF based matrix with good antibacterial properties, which could be used as an ideal antibacterial suture material for urethral reconstruction and other kinds of soft tissue repair [148]. Related studies have further indicated the advantages of hybrid RSF scaffolds for the rapid angiogenesis and effective urethral reconstruction.

4.2.2. Nerve regeneration

Nerve defects such as peripheral nerve injuries could lead to a serious loss of sensation or motor control and even lifelong disability. In general,

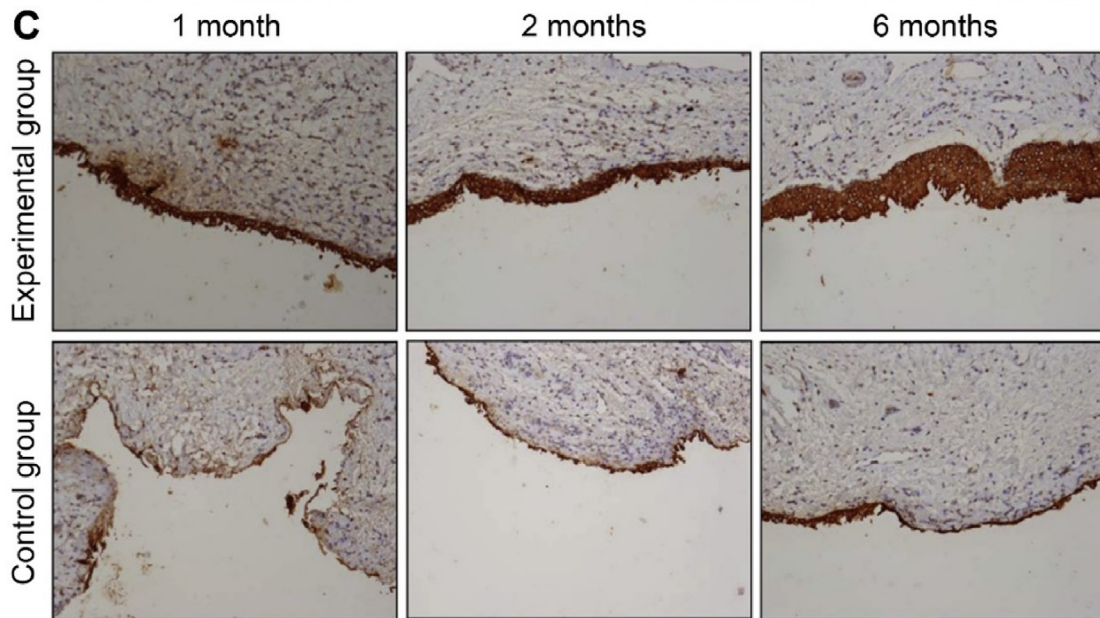
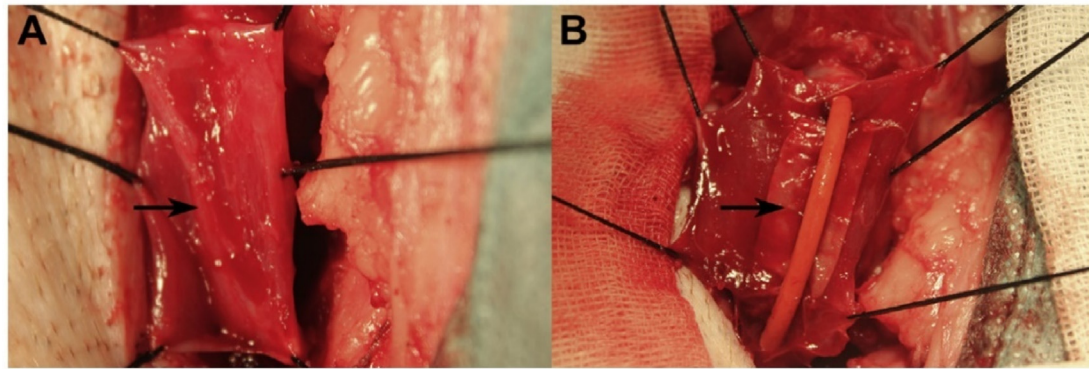
when the defect gaps are longer than 2 cm, it has been reported that the peripheral nervous system could not undergo spontaneous regeneration [149,150]. Until now, tissue engineering method using the combination of cells, artificial scaffolds, and suitable growth factors becomes a potential approach to the treatment of longer nerve damage.

Collaborated by Song et al., Zhang's group fabricated a kind of aligned SF-based scaffolds *via* electrospinning aimed at peripheral nerve regeneration [151]. At the same time, active growth factors such as brain-derived neurotrophic factor (BDNF) and vascular endothelial growth factor (VEGF) were simultaneously loaded into the scaffolds for sustained release. Herein, SF aqueous solution was introduced to mix with growth factors as electrospinning dope, which could well maintain the bioactivity of BDNF and VEGF. The biodegradability of RSF material also makes it feasible for sustained release of the loaded growth factors. Results indicated that the dual factor-loaded aligned electrospun RSF microfibrous scaffolds promoted Schwann cell spread and proliferation *via in vitro* cell studies, and enhanced the neovascularization in a mouse model *via* subcutaneous implantation [151]. Interestingly, in the ongoing studies of the same research group, two different aligned scaffolds consisting of coaxial electrospun RSF fibers were further fabricated by switching the position of the BDNF and VEGF in either core or shell domain of the RSF fibers [31], as schematically illustrated in Fig. 11D. In order to further demonstrate the clinical potential of the factor-loaded RSF scaffolds, *in vivo* studies about the repairing of peripheral nerve defects like cavernosal nerve injury have been performed (see Fig. 11E–F). Results illustrated that the inner-BDNF/outer-VEGF (IBOV) scaffolds have significantly improved performance for cavernous nerve regeneration than that of the inner-VEGF/outer-BDNF (IVOB) scaffolds, as higher vessel density and positive contents of nerve fibers were both found in group IBOV (see Fig. 11G–H) [31]. This study indicated that reasonable release order could significantly improve the synergistic effect of the dual factors in the unique RSF fiber mats, thus also provided valuable reference for the scaffold design and tissue reconstruction of other tissues.

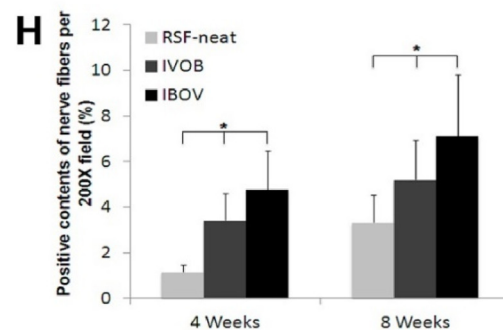
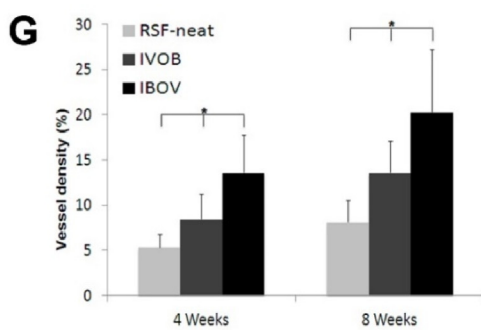
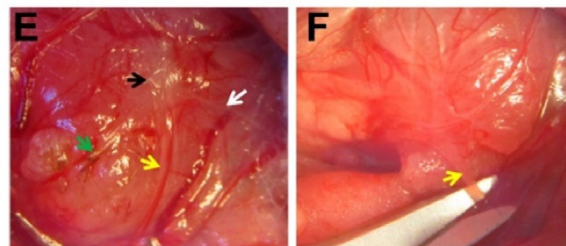
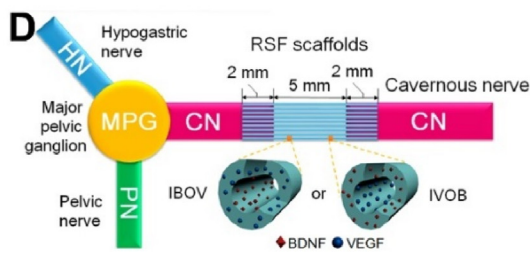
Except for the peripheral nerve repair, SF based biomaterials have also been tried to induce the regeneration of central nerves. For example, Wang et al. have developed a SF/alginate (SF/Alg) composite scaffold enriched with or without nerve growth factor (NGF) by freeze-drying strategy for the treatment of spinal cord injury (SCI). It indicated that the NGF released from Alg microspheres on the SF/Alg scaffold to the central lesion site of SCI significantly enhanced the sparing of spinal cord tissue and increased the number of surviving neurons in a rat model. Moreover, the motor function of rat treated by SF/Alg/NGF was obviously improved compared with the pure SF group [152]. Besides, an amniotic epithelial cells loaded SF scaffold have also been used to repair the SCI in a rat model [153]. Results showed that the cell-scaffold complex resulted in a smaller glial scar in the damaged spinal cord tissue and a marked improvement in motor function than that treated with pure SF scaffolds. These optimal multi-disciplinary approaches of combining SF biomaterials, seeding cells and bioactive factors also offered a promising treatment for the injured central nerves [152–154].

In addition, by decorating the RSF films with integrin-binding peptide motifs (such as YIGSR and GYIGSR) through physical adsorption or covalent modification, Manchineella et al. have investigated their application potential in nerve regeneration [17]. Results showed that covalently functionalized RSF films with GYIGSR could well enhanced hMSCs proliferation and pluripotent maintenance. While in the presence of retinoic acid, this kind of GYIGSR modified RSF films could also significantly promoting differentiation of hMSCs into matured neuron-like cells [17]. The observed morphological changes of the differentiated cells could be further confirmed by the up-regulation of neuronal specific gene expression of MAP2, TUBB3, and NEFL [17]. This kind of GYIGSR modification *via* covalent binding provided another valuable strategy for enhancing the potential of SF based materials for the neural defect therapy.

Urethral regeneration



Nerve regeneration



(caption on next page)

Fig. 11. SF based matrices used for typical soft tissue regeneration. (A) A piece of urethra mucosa (about 3 cm × 1 cm) was excised (black arrow) for the construction of canine urethra defect model. (B) Tissue-engineered mucosa base on stretched electrospun silk fibroin matrices (SESFMs) was positioned into the urethra defect and an F8 catheter was inserted into the urethra (black arrow). (C) Micrographs of the histologic staining (AE1/AE3 IHC) of corresponding urethra tissue (200 ×). (D) Schematic illustration of the suturing of the aligned and growth factor loaded RSF matrices and two cavernous nerve (CN) end. (E) Gross view of the implantation of RSF matrices in rat model. Exposed major pelvic ganglion (MPG, black arrow), pelvic nerve (PN, green arrow), hypogastric nerve (HN, white arrow) and CN (yellow arrow). (F) Gross view of the implantation of RSF matrices in rat model. Establishing CN gap (yellow arrow) with a length of 5 mm using scissors. (G) Statistical results of the vessel densities from corresponding immunohistochemical staining micrographs. (H) Statistical results of the NF-200 positive contents of cavernous nerve fibers from corresponding immunohistochemical staining micrographs. “*”: $p < 0.05$. Images (A)–(C) were reproduced with permission [139]. Copyright 2013, Elsevier Ltd. Images (D)–(H) were modified with permission [31]. Copyright 2016, American Chemical Society.

4.2.3. Liver regeneration

As for acute or chronic liver failure, liver transplantation is a very effective treatment. However, its clinic application is seriously limited by the scarcity of liver donor, immune rejection, and huge costs. As an alternative treatment, stem cell based liver regeneration offers possibilities to overcome the above-mentioned limitations, while it's hard to find a suitable environment that allows the stem cells to develop toward hepatic differentiation and finally forms a functional implant liver construct. So, the development of an ideal scaffold with proper micro-environment for liver regeneration is urgently needed.

In this research field, Xu et al. constructed a MSCs-loaded RSF matrices, as an alternative SF based graft for the treatment of acute liver failure [155]. In this literature, the *in vivo* performance of MSCs-loaded RSF complex was carefully validated in a CCl₄ (carbon tetrachloride) induced fulminant hepatic failure model in mouse. It founded that the MSCs exhibited good cytocompatibility on the electrospun RSF matrices and could feasibly differentiated to hepatocyte-like cells in the hepatocyte culture medium. Moreover, corresponding RSF scaffolds helped the MSCs locate on the surface of the injured liver location over 3 months *in vivo*, which was confirmed by the tracing agents of CM-Dil. The long-term survival and growth of the stem cells in the electrospun RSF scaffolds might contribute to the liver regeneration by secreting some important cytokines and ECM components [155]. Further careful evaluation illustrated that the neovascularization was successfully developed in RSF matrix at the initial stage, and a bile canaliculi-like structure and some hepatocyte-like cells were gradually developed at the following stage in the injure location, which proved the effective liver regeneration property of the stem cell loaded RSF matrices [155]. This impressive research has illustrated that with the help of proper electrospun RSF matrices, the MSCs loaded complex matrices present great application potential for liver repair in the situation of chronic liver injury or acute liver failure.

In addition, the RSF materials have also been used to construct artificial liver model. For example, Abbott et al. demonstrated the suitability of SF lyophilized scaffolds to support the growth and differentiation of HepaRG cell, which is a commonly used cell line to produce hepatic progenitor cell and hepatocyte [156]. Results of the lipid droplet accumulation and expression of steatosis-related genes after exposure to oleic acid showed that the matrix support fabricated by 3% SF combined with HepaRG cells could be suitable for the construction of steatosis liver model [156]. By using a complex RSF scaffold fabricated by blending mulberry (*Bombyx mori*) SF with cell adhesion motif contained non-mulberry (*Antheraea assamensis*) SF, Janani et al. generated a functional liver construct *in vitro*, which enhanced liver-specific functions of cultured hepatocytes according to the evaluation of albumin synthesis, urea synthesis and cytochrome P450 enzyme activity [157,158]. This kind of complex RSF scaffold offers a suitable microenvironment by influencing spheroidal growth of hepatocytes with enhanced biological activity. In summary, these explorations provided useful 3D bio-matrix niche for growing functional liver cells, which probably have great application potentials in bioartificial liver construction as well as *in vivo* liver defect repair.

4.3. Flexible bioelectronic device

The inherent properties of silk have offered unique opportunities for the construction of flexible bioelectronic devices. As early as 2009, the

RSF material has been tried to construct flexible electrode in the field of biomedical applications [159,160]. Recently, with the development of the building blocks extraction strategies and material engineering technologies of RSF materials, the SF based flexible bioelectronic devices, such as degradable conformal electronics, transparent conductor, and triboelectric nanogenerators (TEGs) etc. have all achieved rapid development.

4.3.1. Degradable conformal electronic

In order to interface with the curved surfaces of biological systems, traditional flexible devices commonly use elastomeric polymer thin films as substrates, such as poly(ethylene terephthalate) (PET), polyimide (PI), and PDMS films [161]. Compared with these synthetic polymers, the robust mechanical properties together with excellent biocompatibility and processibility make SF an excellent candidate to serve as a degradable and biocompatible supporting and packaging material for flexible bioelectronic devices.

Based on this idea, SF has been firstly attempted as an efficient supporting substrate in flexible bioelectronic devices to transfer active electronic components onto the surfaces of organs with complex shapes, such as the brain [162] and tooth [163], to obtain conformal contact and desirable functions. For example, by integrating single crystalline silicon electronics onto the thin layer of RSF film, Kim et al. [159] firstly attempted and successfully constructed a RSF based flexible bioelectronic devices. This strategy induced a system in which the substrate (RSF film) is water soluble, and resorbable. Corresponding *in vivo* biocompatibility evaluations showed no harmful effects on living animals [159], which further paved the way for its application potential as implantable devices. Based on this pioneer exploration, Kim et al. further developed a flexible electrode material which successfully collected electroencephalogram signals [162]. It demonstrated a type of bio-interfaced system which depends on ultrathin electronics supported by RSF bioresorbable substrates. Mounting such devices on tissue could induce a spontaneous conformal wrapping process driven by capillary forces on the organ surface, then allowing the substrate to dissolve and resorb. Results showed that proper mesh designs and ultrathin forms for the electronics ensure minimal stresses on the tissue and highly conformal coverage, even for complex curvilinear surfaces. As for the evaluation of evoked potential response on the brain, the 2.5 μm mesh electrode showed the best performance [162].

The above mentioned conformal electronic are all use the SF component as water-dissolvable biointerfaces. Recently, with the development of the material engineering strategies, RSF substrate with high flexibility have been achieved, thus further speed up the development of RSF based conformal electronic. For example, Patil et al. firstly realized a nontransient (water insoluble) and flexible SF bionic interfaces for direct electrical recording of neural activity from the peripheral nerves or the cortex [164], as shown in Fig. 12A–C. This platform exploit SF as the organic foundation of a new class of implantable RSF based devices that are nontransient, flexible and conformal to target tissue morphologies. In this literature, a conducting layer is keeping in between two thin RSF layers (about 15 μm in thickness), which served as the substrate and the insulation, see Fig. 12A. In addition, this kind of silk ‘sandwich’ sensor also employed a bilayer bandage of resorbable SF and biocompatible elastomer to facilitate quick conformal on the tissue surfaces in a suture-free manner [164]. In addition, a stretchable silk hydrogel

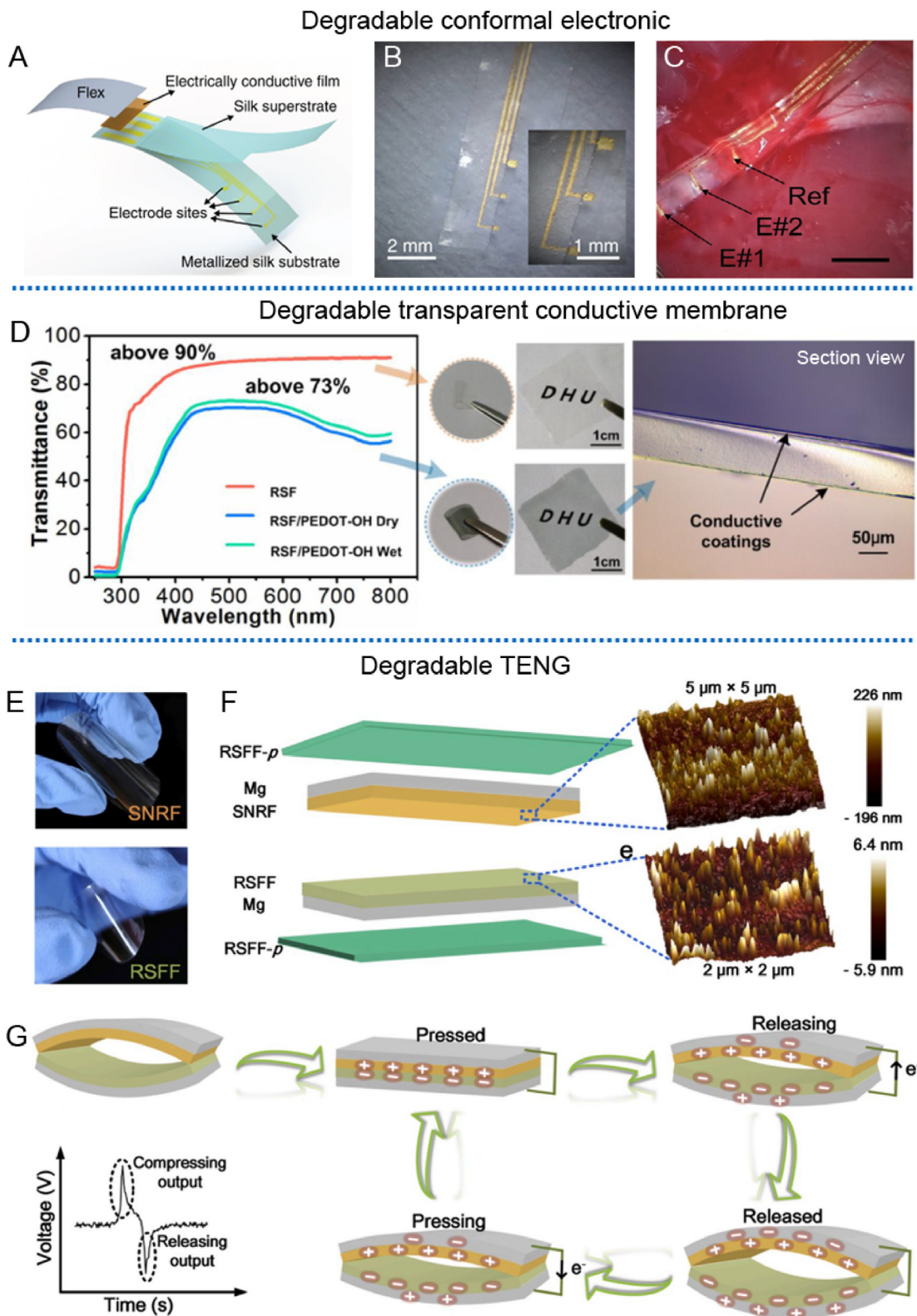


Fig. 12. Typical applications of SF based material as flexible bioelectronic devices. (A) Schematic presentation of the construction of a flexible SF based conformal electronic. (B) Photographs of the fabricated conformal electronic (with two recording channels and one reference channel) (C) Photograph of the conformal electronic deployed as a band-aid on the sciatic nerve of a rat to collect neuroelectric signals (scale bar = 2 mm). (D) A SF based transparent conductive RSF/PEDOT–OH film with good transparency and conductivity. (E) Gross view of the SNRF and RSFF. (F) Schematic illustration of TENG's structure and the AFM images of friction layers (Mg coated SNRF and RSFF). (G) Schematic presentation of the working mechanism of corresponding TENG and the typical output voltage signal during one stimulation cycle. Images (A–C) were modified with permission [164]. Copyright 2020, Elsevier Ltd. Image (D) was reproduced with permission [166]. Copyright 2021, American Chemical Society. Images (E–G) were reproduced with permission [41]. Copyright 2020, Elsevier Ltd.

electrode based on PEGylated SF and PEDOT:PSS has also been reported by Cui et al. [165]. It demonstrated that the PEGylated silk protein with poly(ethylene glycol) diglycidyl ether (PEGDE) had significantly improved the Young's modulus and stretchability of the hydrogel compared to traditional silk hydrogel, and hence realized a stretchable, nontransient, and relative stable conformal electronic for neural activity characterization [165]. These developed technologies allowed intimate integration of finely spaced flexible electrode systems with living organ, achieving the kind of reliable biotic/abiotic interface connections, thus presented great potential on human health monitoring and electrical stimulation.

4.3.2. Degradable transparent conductive film

Desirable transparency and conductivity of the flexible film could allow real-time observation of live cells under electrical stimulation and hence provided an idea platform for the revealing of cell-material interaction and electrical stimulation on cell behaviors. In addition, due to the promoting effect of electrical stimulation on nerve regeneration, this kind of biodegradable flexible conductor also exhibit good potential for nerve repair.

By using SF, poly(3,4-ethylenedioxythiophene) (PEDOT) and its derivative materials, Zhuang et al. have constructed and developed a few kinds of SF based flexible conductive films [26,166]. In the initial exploration, by using ammonium persulfate (APS) as oxidant, hydroxymethyl-3,4-ethylenedioxythiophene (EDOT-OH) had been polymerized and deposited on the surface of RSF film. For the sake of improving the efficiency of this deposition, sodium dodecyl sulfate (SDS) was adopted as surfactant to construct a well-organized and stable poly(hydroxymethyl-3,4-ethylenedioxythiophene (PEDOT-OH) coating on RSF film and finally a conductive RSF/PEDOT-OH film was produced [26]. This biodegradable conductive film exhibited a sheet resistance (R_s) of about $3.28 \times 10^5 \Omega/\text{sq}$ and corresponding conductivity of about $6.1 \times 10^{-3} \text{ S/cm}$. Moreover, favorable electrochemical stability and good cytocompatibility of PC12 cells of the fabricated film were also demonstrated [26]. The conductivity and transparency are both quite important in the field of live cell observation and cell-material interaction revealing. To reasonably trade-off the transparency and conductivity of the PEDOT-OH coating on RSF film, a composite oxidants recipe of FeCl_3 and APS was developed [166]. Probably because of the Fe^{3+} regeneration through APS and the electrostatic interaction from oppositely charged doping ions in PEDOT-OH, structural defects and excessive deposition of the conductive coating layer were both avoided [166]. As a result, a well-organized nanoscale conductive coating obtained, inducing a relative transparent conductive RSF/PEDOT-OH film, see Fig. 12D. Whereas, the mentioned coating was difficult to be achieved in traditional single oxidant system. Using this developed process, the produced film performed a R_s of $5.12 \times 10^4 \Omega/\text{sq}$, a conductivity of $8.9 \times 10^{-2} \text{ S/cm}$, and a transmittance over 70% at maximum in the visible light range, as shown in Fig. 12D. Furthermore, the transparent conductive and relative stable RSF/PEDOT-OH film provided a supportive environment for adhesion, growth, and effective electrical stimulation of cells. In addition, an one-step facile PEDOT:PSS modification approach for RSF film based on conformation transformation and embedding of macromolecules (PEDOT:PSS) was further developed to fabricate transparent conductive RSF/PEDOT:PSS film [27]. The feasibility of real-time observation of cell adhesion was successfully achieved on these transparent conductive films [27,166]. This kind of biodegradable conductive and transparent flexible film has become an ideal candidate as stimulation electrode for cell-material interaction revealing, tissue engineering and further biomedical applications.

4.3.3. Degradable TENG and conductive wire

The research about implantable self-powered electronic devices and wires with good biocompatibility and biodegradability presents significant values. It is well known that TENGs can convert the mechanical energy to electrical energy, and hence power other electric devices.

However, for implant biomedical applications, it's a challenge to fabricate the fully biodegradable TENGs with excellent output performance and high sensitivity. The excellent inherent properties of SF have made it a potential material to fabricate flexible energy devices.

Recently, Niu et al. have firstly extracted SNRs, a unique building blocks with retained inherent silk structures [13,41], as already mentioned in section 2.3. Based on these developed extraction strategies, a novel RSF based TENG was constructed using SF nanoribbon film (SNRF) and RSF film (RSFF) with different crystalline structures [41], as presented in Fig. 12E–F. Own to the different secondary structures, crystallinity, and work functions of SNRF and RSFF, they were used as friction layers to construct all SF based TENG. During the process of applying and removing external mechanical force, the electrons transferred from SNRF to RSFF, and hence produced electrical energy [41], as shown in Fig. 12G. It was reported that under a 100 M Ω load resistance, the optimal output voltage and power density of the all SF based TENG are 41.6 V, and 86.7 mW m $^{-2}$, respectively. In addition, this SNRF/RSFF TENG could realize real-time monitoring the tiny motions of varied body parts, such as finger taping, footsteps, elbow motion, and even a human pulse, without the need of an external power source [41]. Compared with other fully biodegradable TENGs, this SNRF/RSFF TENG presented greater output performance and higher sensitivity [41,167]. Moreover, the friction layers, SNRF and RSFF, have also been proved to have good biocompatibility and biodegradability [41].

Moreover, a flexible and biodegradable conductive wire used together with the above mentioned SNRF/RSFF TENG have also been developed and utilized by the same research group [168]. Firstly, the SNR and konjac glucomannan composite film (SKCF) was prepared by using vacuum filtration and thermal resistance evaporation. Herein, konjac glucomannan (KGM) mainly contributes to the elongation of SKCFs at break and the formula of S8K2 (mass ratio of SNR: KGM = 8 : 2) presents an excellent toughness of 0.6 MJ m $^{-3}$ in wet condition. In order to fabricate degradable conductive wire, S8K2 was coated with a thin layer of Au and then cut into wires with 1 mm in width. This kind of SKCF-Au wire exhibited a resistance of approximately 8 Ω/cm [168]. When integrated the produced SKCF-Au wire with the above mentioned flexible SNRF/RSFF TENG, the highest output power density was achieved as 314.3 mW m $^{-2}$. The output power density of the TENG used SKCF-Au wire was 2.8–4.7 times higher than that of the TENG used traditional Cu wire, Cu foil wire, or Al foil wire [168]. It proved that this flexible and biodegradable conducting wire could effectively transfer the generated power from SF based TENG. In addition, cells showed good cytocompatibility both on the SKCF and SKCF-Au surfaces. Herein, the percentage of biodegradable component in the integrated energy device (TENG and corresponding wires) is over 99.9%, and this developed integrated energy device could be thought as fully biodegradable device.

The almost fully biodegradable SF based flexible bioelectronic devices, such as conformal electronics, transparent conductive film, energy generating devices and corresponding conductive wires prepared based on the extracted building blocks of silk have presented outstanding conductive performance and even realized the pulse-driven self-power. The fabricated conformal electronics and electrode material ensure minimal stresses on the tissue and highly conformal coverage, even for complex curvilinear surfaces. The constructed transparent conductor performed good conductively, electrochemical stability, and feasibly achieved real-time observation of the electrical stimulation process of cells. All the constructed SF based flexible bioelectronic devices showed promising application potentials in the fields of biodegradable electrode, cell-electrical stimulation interactions, nerve tissue engineering and biosensing.

5. Future perspectives

At present, SF has been regarded as an excellent raw material for a variety of emerging biomedical applications beyond its traditional role in textiles and sutures. However, many researches about the desired

building block extraction, controllable building blocks reconstruction and related biomedical applications are still on their infant stage, further detailed and in-depth investigations are required, at least along the following lines, in our opinion.

Development of bioinspired building blocks extraction and related reconstruction strategies: Until now, it is undoubtedly that SF based biomaterials that meet different morphology and formats needs can be obtained by various fabrication strategies. However, the extraction of building blocks or preparation of SF based biomaterials often requires complex processes or expensive reagents, and it is difficult to reserve satisfied comprehensive properties while meeting a specific performance requirement. Therefore, to feasibly obtain biomaterials with satisfied comprehensive properties and desired functions, the construction of RSF biomaterials still face many challenges. On the one hand, the extraction strategies of building block which retained critical primitive characteristics of the hierarchical natural silk are urgently needed, especially the method with green and controllable properties. On the other hand, the construction strategies of SF based biomaterials with bioinspired multi-level structures are also quite important to solve the challenge issues. On this challenging topic, Niu et al. have recently extracted a unique building blocks (SNR) which retained partial secondary structural basis of silk by using TEMPO/NaBr/NaClO solvent system, and further constructed a novel RSF film with much better cytocompatibility and almost fully biodegradable RSF based TENG with good comprehensive properties by using this building blocks and proper material processing and combination technologies [41,168]. So, for widely and effectively usage of SF based biomaterials, both the building blocks extraction and corresponding reconstruction strategies are quite important directions to be further developed.

Effective bioinspired modification of SF materials: Unlike the fibrous component in ECM, most of the SF was extracted from *Bombyx mori*, which lacks the component of specific amino acid sequences as ligand for enhancing specific cell adhesion, such as RGD, REDV, YIGSR, GYIGSR etc. So, as for most of the biomedical application of RSF materials, the cell adhesion ability is relatively poor than that of the fibronectin, laminin, and collagen with the same material formats. In order to compensate for this shortcoming, some modification strategies such as chemical grafting and genetic engineering strategies have been attempted. These kind of bioinspired modification methods are probably quite effective for improving the biomedical performance for cell culture and tissue repair. Another example would be intrinsically luminescent silk materials produced through genetic engineering or altering the food of silkworms [169–176], which are useful for special biomedical usage. In addition, improved cytocompatibility, conductivity and mechanical properties, such as elastomeric properties and stretchability, may also be achieved through chemical or physical modification progress. It is envisaged that, through such specific modifications, the biointegrated flexible devices could be endowed with even more feasible construction progress and interesting functionalities. Lastly, by using the developed recombinant DNA technology [7,177], silks could be rationally designed and synthesized via genetic control. The modification at gene level provides a powerful tool to construct silk protein with desired amino acid sequence and high degree of molecular definition, and hence could provide excellent comprehensive properties.

Combination of unique technologies to reveal more cell–material interactions: Design of effective biomaterials is, in a large extent, dependent upon the comprehensive understanding of the cell–material interactions. An important advantage of SF is that it is easy to prepare for various material formats. Combination with the non-fouling modification and surface patterning technologies, the convenience in preparing topological features and fiber materials has made RSF material a potential model for the basic study of cell–material interactions, such as the surface chemical and physical cues, inherent fiber diameter and corresponding arrangement effects on cell behaviors. Moreover, compared with the widely studied static material cues, the researches on the dynamic material cues effect on cell behaviors are still relatively scarce,

which is closely related to the difficulty of the construction and regulation of dynamic material microenvironments. SF hydrogel has good biocompatibility, which can occur protein conformation transition [178] and protein degradation [23,179], thus could be used for mimicking the dynamical behaviors of ECM. These dynamic processes will obviously bring out dynamic changes of material volume, pore size and stiffness [95,96], and hence provided potential models for constructing 3D dynamic material microenvironment feasible for cell studies. Such as revealing these dynamic material cues effect on cell adhesion, proliferation, and differentiation. Related fundamental studies are expected to expand the understanding of the cell–material interactions. The new insight could also be quite helpful for guiding the development of novel RSF and non-RSF biomaterials.

Biodegradable and flexible bioelectronic devices: a concept and a practice: The concept of biodegradable and flexible bioelectronic devices is extremely useful in the field of disease detection and therapy. As for the flexible, biocompatible and biodegradable nature, the silk has become one of the most promising raw materials for the construction of biodegradable and flexible bioelectronic devices. The past decade has witnessed the emergence of varied SF based rudiment bioelectronics for wide biomedical applications, such as signal monitoring, biosensing, brain–machine interfaces, as well as memory devices [180–184]. To obtain practical application, this research field is still confronted with many fundamental and technical challenges to be addressed. Such as the SF based biodevices are all reconstructed from the extracted building blocks of silk, there is still a big gap of mechanical properties such as flexibility between reconstructed RSF materials and natural silk. In addition, even though the excellent dielectric property of SF makes RSF films suitable for being utilized as passive substrates and dielectric layers in flexible bioelectronic devices, related devices still inevitably require metal or conducting polymers as conductive components, thus limiting their biodegradability and bioresorbability to some extent for applications in biological systems.

Accelerating animal and clinical trials: Until now, majority of the reports about the biomedical applications of RSF materials are still focused on the *in vivo* or small animal experiments, thus the results may not fully be extended for human use. In order to evaluate their actual clinical and commercial value, and accelerating the process from basic research to clinical application, big animal model experiments such as pig or monkey, and even human clinical trials are urgently called for. More evaluations are needed to be performed in the future to identify the specific requirements of using SF based materials or devices in clinical trials and constructing bioinspired component and structures. Such valuable explorations and researches will not only indicate the correct develop directions but also provide full confidence for the development of other kinds of silk biomaterials.

Assurance of the quality stability of raw materials: As a natural material, the raw silk will inevitably meet the problems such as quality instability between batches, which might limit parts of its commercial applications. On the one hand, developing stable and controllable initial breeding process and conditions, such as automatic large-scale farming of *Bombyx mori* may reduce the fluctuation of unstable quality to a certain extent. On the other hand, the development of mild and controllable extraction strategies could provide controllable building blocks of silk with constant quality, such as the molecular weight and segment length. These useful strategies are all efficiency to control the quality stability of the raw materials, and hence assurance corresponding SF based biomaterials quality and function, finally make it feasible to become stable commercial products.

6. Conclusions

The combination of robustness mechanical properties, excellent biocompatibility, processability and modifiability make the SF materials transformed fields ranging from fundamental research in cell–material interactions to applications in varied biomedical fields. The bioinspired

indirect construction strategies indeed give SF excellent processability and modifiability, thus well meet the diversified needs in biomedical applications. From these perspectives, this review systematically introduced typical building blocks of silk at different levels, focusing on the useful and novel extraction methods (top-down). Then, the developed powerful construction strategies (bottom-up) for functional RSF biomaterials were also summarized, as well as their recent advances in corresponding biomedical applications, especially in the fields of cell-material interactions, soft tissue regeneration, and flexible bio-electronic devices. Corresponding bioinspired strategies and effective biomedical applications could afford valuable references for the design and modification of functional RSF biomaterials, and further promote the high-quality-utilization of natural silk or other biomass materials. Moreover, further improvement of the challenging building blocks extraction and material processing techniques and associated investigations of the biomedical applications both *in vitro* and *in vivo* would provide effective biomaterial or biodevice for the monitoring and treatment of disease. Related potential opportunities afforded by the bioinspired SF biomaterials could reshape the future material processing strategies toward environmentally friendly and sustainability, motivating the production of high-performance deliverables that could raise a revolutionary influence on both the scientific community and society.

Declaration of competing interest

The authors declare that they have no known competing financial interests or personal relationships that could have appeared to influence the work reported in this paper.

Acknowledgments

This work was financially supported by the Natural Science Foundation of Shanghai (20ZR1402400), the National Natural Science Foundation of China (52173031, 51903045, 51703033), the Program of Shanghai Academic/Technology Research Leader (20XD1400100), the National Key Research and Development Program of China (2018YFC1105802), the Basic Research Project of the Science and Technology Commission of Shanghai Municipality (21JC1400100), the International Cooperation Fund of the Science and Technology Commission of Shanghai Municipality (19520744500), and the Fundamental Research Funds for the Central Universities (2232020D-04, 2232019A3-06, 2232019D3-02).

References

- [1] F.G. Omenetto, D.L. Kaplan, New opportunities for an ancient material, *Science* 329 (2010) 528–531, <https://doi.org/10.1126/science.1188936>.
- [2] D.N. Rockwood, R.C. Preda, T. Yucel, X. Wang, M.L. Lovett, D.L. Kaplan, Materials fabrication from *Bombyx mori* silk fibroin, *Nat. Protoc.* 6 (2011) 1612–1631, <https://doi.org/10.1038/nprot.2011.379>.
- [3] L.D. Koh, Y. Cheng, C.P. Teng, Y.W. Khin, X.J. Loh, S.Y. Tee, M. Low, E. Ye, H.D. Yu, Y.W. Zhang, M.Y. Han, Structures, mechanical properties and applications of silk fibroin materials, *Prog. Polym. Sci.* 46 (2015) 86–110, <https://doi.org/10.1016/j.progpolymsci.2015.02.001>.
- [4] J. Melke, S. Midha, S. Ghosh, K. Ito, S. Hofmann, Silk fibroin as biomaterial for bone tissue engineering, *Acta Biomater.* 31 (2016) 1–16, <https://doi.org/10.1016/j.actbio.2015.09.005>.
- [5] C. Vepari, D.L. Kaplan, Silk as a biomaterial, *Prog. Polym. Sci.* 32 (2007) 991–1007, <https://doi.org/10.1016/j.progpolymsci.2007.05.013>.
- [6] G.H. Altman, F. Diaz, C. Jakuba, T. Calabro, R.L. Horan, J.S. Chen, H. Lu, J. Richmond, D.L. Kaplan, Silk-based biomaterials, *Biomaterials* 24 (2003) 401–416, [https://doi.org/10.1016/s0142-9612\(02\)00353-8](https://doi.org/10.1016/s0142-9612(02)00353-8).
- [7] W.W. Huang, S.J. Ling, C.M. Li, F.G. Omenetto, D.L. Kaplan, Silk worm silk-based materials and devices generated using bio-nanotechnology, *Chem. Soc. Rev.* 47 (2018) 6486–6504, <https://doi.org/10.1039/c8cs00187a>.
- [8] G. Guidetti, L. d'Amone, T. Kim, G. Matzeu, L. Moga-Soldevila, B. Napier, N. Ostrovsky-Snyder, J. Roshko, E. Ruggeri, F.G. Omenetto, Silk materials at the convergence of science, sustainability, healthcare, and technology, *Appl. Phys. Rev.* 9 (2022), 011302, <https://doi.org/10.1063/5.0060344>.
- [9] S.Z. Zou, S.N. Fan, A.L. Oliveira, X. Yao, Y.P. Zhang, H.L. Shao, 3D printed gelatin scaffold with improved shape fidelity and cytocompatibility by using *Antheraea pernyi* silk fibroin nanofibers, *Adv. Fiber Mater.* 4 (2022) 758–773, <https://doi.org/10.1007/s42765-022-00135-w>.
- [10] Q. Zhang, K.Q. Wang, M.Q. Zhang, T. Chen, L.Y. Li, S.H. Shi, R.Y. Jiang, Electronic structure optimization boosts Pd nanocrystals for ethanol electrooxidation realized by Te doping, *CrystEngComm* (2022), <https://doi.org/10.1039/d2ce00710j>.
- [11] Q. Zhang, M.Q. Zhang, T. Chen, L.Y. Li, S.H. Shi, R.Y. Jiang, Unconventional phase engineering of fuel-cell electrocatalysts, *J. Electroanal. Chem.* 916 (2022), 116363, <https://doi.org/10.1016/j.jelechem.2022.116363>.
- [12] Q. Zhang, F. Yue, L.J. Xu, C.X. Yao, R.D. Priestley, S.F. Hou, Paper-based porous graphene/single-walled carbon nanotubes supported Pt nanoparticles as freestanding catalyst for electro-oxidation of methanol, *Appl. Catal., B* 257 (2019), 117886, <https://doi.org/10.1016/j.apcatb.2019.117886>.
- [13] Q.Q. Niu, Q.F. Peng, L. Lu, S.N. Fan, H.L. Shao, H.H. Zhang, R.L. Wu, B.S. Hsiao, Y.P. Zhang, Single molecular layer of silk nanoribbon as potential basic building block of silk materials, *ACS Nano* 12 (2018) 11860–11870, <https://doi.org/10.1021/acsnano.8b03943>.
- [14] H.J. Jin, D.L. Kaplan, Mechanism of silk processing in insects and spiders, *Nature* 424 (2003) 1057–1061, <https://doi.org/10.1038/nature01809>.
- [15] A.D. Malay, R. Sato, K. Yazawa, H. Watanabe, N. Ifuku, H. Masunaga, T. Hikima, J. Guan, B.B. Mandal, S. Damrongsakul, K. Numata, Relationships between physical properties and sequence in silkworm silks, *Sci. Rep.* 6 (2016), 27573, <https://doi.org/10.1038/srep27573>.
- [16] S. Ketten, Z.P. Xu, B. Ihle, M.J. Buehler, Nanofinements controls stiffness, strength and mechanical toughness of beta-sheet crystals in silk, *Nat. Mater.* 9 (2010) 359–367, <https://doi.org/10.1038/nmat2704>.
- [17] S. Manchineella, G. Thirivikraman, B. Basu, T. Govindaraju, Surface-functionalized silk fibroin films as a platform to guide neuron-like differentiation of human mesenchymal stem cells, *ACS Appl. Mater. Interfaces* 8 (2016) 22849–22859, <https://doi.org/10.1021/acsmi.6b06403>.
- [18] D. Kochhar, M.K. DeBari, R.D. Abbott, The materiobiology of silk: exploring the biophysical influence of silk biomaterials on directing cellular behaviors, *Front. Bioeng. Biotechnol.* 9 (2021), 697981, <https://doi.org/10.3389/fbioe.2021.697981>.
- [19] L.W. Tien, E.S. Gil, S.H. Park, B.B. Mandal, D.L. Kaplan, Patterned silk film scaffolds for aligned lamellar bone tissue engineering, *Macromol. Biosci.* 12 (2012) 1671–1679, <https://doi.org/10.1002/mabi.201200193>.
- [20] S. Madduri, M. Papaloizos, B. Gander, Trophically and topographically functionalized silk fibroin nerve conduits for guided peripheral nerve regeneration, *Biomaterials* 31 (2010) 2323–2334, <https://doi.org/10.1016/j.biomaterials.2009.11.073>.
- [21] C.C. Ai, L. Liu, J.C.H. Goh, Pore size modulates *in vitro* osteogenesis of bone marrow mesenchymal stem cells in fibronectin/gelatin coated silk fibroin scaffolds, *Mater. Sci. Eng. C* 124 (2021) 112088, <https://doi.org/10.1016/j.msec.2021.112088>, 112088.
- [22] P. Edwin, N.R. Rajagopalan, S.K. Bajpai, Morphology and cellular-traction of fibroblasts on 2D silk-fibroin hydrogel substrates, *Soft Mater.* 20 (2022) 45–56, <https://doi.org/10.1080/1539445x.2021.1918719>.
- [23] C.C. Guo, C.M. Li, D.L. Kaplan, Enzymatic degradation of *Bombyx mori* silk materials: a review, *Biomacromolecules* 21 (2020) 1678–1686, <https://doi.org/10.1021/acs.biomac.0c00090>.
- [24] J. Wang, Y.P. Chen, G.S. Zhou, Y.Y. Chen, C.B. Mao, M.Y. Yang, Polydopamine-coated *Antheraea pernyi* (A. pernyi) silk fibroin films promote cell adhesion and wound healing in skin tissue repair, *ACS Appl. Mater. Interfaces* 11 (2019) 34736–34743, <https://doi.org/10.1021/acsmi.9b12643>.
- [25] X.W. Wang, Y. Gu, Z.P. Xiong, Z. Cui, T. Zhang, Silk-molded flexible, ultrasensitive, and highly stable electronic skin for monitoring human physiological signals, *Adv. Mater.* 26 (2014) 1336–1342, <https://doi.org/10.1002/adma.201304248>.
- [26] A. Zhuang, Y.J. Bian, J.W. Zhou, S.N. Fan, H.L. Shao, X.C. Hu, B. Zhu, Y.P. Zhang, All-organic conductive biomaterial as an electroactive cell interface, *ACS Appl. Mater. Interfaces* 10 (2018) 35547–35556, <https://doi.org/10.1021/acsmi.8b13820>.
- [27] A. Zhuang, X.Y. Huang, S.N. Fan, X. Yao, B. Zhu, Y.P. Zhang, One-step approach to prepare transparent conductive regenerated silk fibroin/PEDOT:PSS films for electroactive cell culture, *ACS Appl. Mater. Interfaces* 14 (2022) 123–137, <https://doi.org/10.1021/acsmi.1c16855>.
- [28] P. Bhattacharjee, B. Kundu, D. Naskar, H.W. Kim, T.K. Maiti, D. Bhattacharya, S.C. Kundu, Silk scaffolds in bone tissue engineering: an overview, *Acta Biomater.* 63 (2017) 1–17, <https://doi.org/10.1016/j.actbio.2017.09.027>.
- [29] W.Z. Sun, D.A. Gregory, M.A. Tomeh, X.B. Zhao, Silk fibroin as a functional biomaterial for tissue engineering, *Int. J. Mol. Sci.* 22 (2021) 1499, <https://doi.org/10.3390/ijms22031499>.
- [30] P. Gupta, B.B. Mandal, Silk biomaterials for vascular tissue engineering applications, *Acta Biomater.* 134 (2021) 79–106, <https://doi.org/10.1016/j.actbio.2021.08.004>.
- [31] Y.P. Zhang, J.W. Huang, L. Huang, Q.Q. Liu, H.L. Shao, X.C. Hu, L.J. Song, Silk fibroin-based scaffolds with controlled delivery order of VEGF and BDNF for cavernous nerve regeneration, *ACS Biomater. Sci. Eng.* 2 (2016) 2018–2025, <https://doi.org/10.1021/acsbomaterials.6b00436>.
- [32] B.B. Mandal, A. Grinberg, E.S. Gil, B. Panilaitis, D.L. Kaplan, High-strength silk protein scaffolds for bone repair, *Proc. Natl. Acad. Sci. USA* 109 (2012) 7699–7704, <https://doi.org/10.1073/pnas.1119471109>.
- [33] H.J. Jin, J. Park, V. Karageorgiou, U.J. Kim, R. Valluzzi, D.L. Kaplan, Water-stable silk films with reduced beta-sheet content, *Adv. Funct. Mater.* 15 (2005) 1241–1247, <https://doi.org/10.1002/adfm.200400405>.

- [176] Z. Guo, Y. Chi, W. Xie, J. Lu, D. Wang, F. Gao, G. Zhang, Q. Feng, H. Wu, L. Zhao, Synergetic enhancement of mechanical properties for silk fibers by a green feeding approach with nano-hydroxyapatite/collagen composite additive, *J. Nat. Fibers* (2021), <https://doi.org/10.1080/15440478.2021.1875372>.
- [177] T. Deptuch, H. Dams-Kozłowska, Silk materials functionalized via genetic engineering for biomedical applications, *Materials* 10 (2017) 1417, <https://doi.org/10.3390/ma10121417>.
- [178] R. Ziadlou, S. Rotman, A. Teuschl, E. Salzer, A. Barbero, I. Martin, M. Alini, D. Eglin, S. Grad, Optimization of hyaluronic acid-tyramine/silk-fibroin composite hydrogels for cartilage tissue engineering and delivery of anti-inflammatory and anabolic drugs, *Mater. Sci. Eng. C* 120 (2021), 111701, <https://doi.org/10.1016/j.msec.2020.111701>.
- [179] Q. Lu, B. Zhang, M.Z. Li, B.Q. Zuo, D.L. Kapan, Y.L. Huang, H.S. Zhu, Degradation mechanism and control of silk fibroin, *Biomacromolecules* 12 (2011) 1080–1086, <https://doi.org/10.1021/bm101422j>.
- [180] Y. Xing, C.Y. Shi, J.H. Zhao, W. Qiu, N.B. Lin, J.J. Wang, X.B. Yan, W.D. Yu, X.Y. Liu, Mesoscopic-functionalization of silk fibroin with gold nanoclusters mediated by keratin and bioinspired silk synapse, *Small* 13 (2017), 1702390, <https://doi.org/10.1002/sml.201702390>.
- [181] G. Chen, N. Matsuhisa, Z.Y. Liu, D.P. Qi, P.Q. Cai, Y. Jiang, C.J. Wan, Y.J. Cui, W.R. Leow, Z.J. Liu, S.X. Gong, K.Q. Zhang, Y. Cheng, X.D. Chen, Plasticizing silk protein for on-skin stretchable electrodes, *Adv. Mater.* 30 (2018), 1800129, <https://doi.org/10.1002/adma.201800129>.
- [182] C.Y. Wang, K.L. Xia, Y.Y. Zhang, D.L. Kaplan, Silk-based advanced materials for soft electronics, *Acc. Chem. Res.* 52 (2019) 2916–2927, <https://doi.org/10.1021/acs.accounts.9b00333>.
- [183] C.M. Li, C.C. Guo, V. Fitzpatrick, A. Ibrahim, M.J. Zwierstra, P. Hanna, A. Lechtig, A. Nazarian, S.J. Lin, D.L. Kaplan, Design of biodegradable, implantable devices towards clinical translation, *Nat. Rev. Mater.* 5 (2020) 61–81, <https://doi.org/10.1038/s41578-019-0150-z>.
- [184] C.Y. Wang, T. Yokota, T. Someya, Natural biopolymer-based biocompatible conductors for stretchable bioelectronics, *Chem. Rev.* 121 (2021) 2109–2146, <https://doi.org/10.1021/acs.chemrev.0c00897>.